OFFICE OF NAVAL RESEARCH

Contract N00014-84-G-0201

Task No. 0051-865

Technical Report #31

Electrochemistry and Spectroelectrochemistry of 1,8-Naphthalene and
1,8-Anthracene-Linked Cofacial Binuclear Metallophthalocyanines.
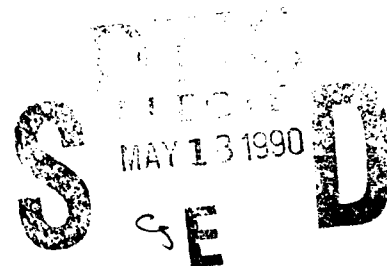New Mixed Valence Metallophthalocyanines

By

N. Kobayashi, H. Lam, W.A. Nevin, P. Janda, C.C. Leznoff and A.B.P. Lever*

in

Inorganic Chemistry

York University
Department of Chemistry, 4700 Keele St., North York
Ontario, Canada   M3J 1P3

90 05 18 009

SECURITY CLASSIFICATION OF THIS PAGE

REPORT DOCUMENTATION PAGE

1a. REPORT SECURITY CLASSIFICATION	1b RESTRICTIVE MARKINGS
2a. SECURITY CLASSIFICATION AUTHORITY Unclassified	3. DISTRIBUTION / AVAILABILITY OF REPORT As it appears on the report
2b. DECLASSIFICATION / DOWNGRADING SCHEDULE	
4 PERFORMING ORGANIZATION REPORT NUMBER(S) Report #31	5. MONITORING ORGANIZATION REPORT NUMBER(S)

6a. NAME OF PERFORMING ORGANIZATION A.B.P. Lever, York University Chemistry Department	6b. OFFICE SYMBOL (If applicable)	7a. NAME OF MONITORING ORGANIZATION Office of Naval Research
6c. ADDRESS (City, State, and ZIP Code) 4700 Keele St., North York, Ontario M3J 1P3 Canada		7b. ADDRESS (City, State, and ZIP Code) Chemistry Division 800 N. Quincy Street Arlington, VA 22217 U.S.A.
8a. NAME OF FUNDING / SPONSORING ORGANIZATION	8b. OFFICE SYMBOL (If applicable)	9 PROCUREMENT INSTRUMENT IDENTIFICATION NUMBER N00014-84-G-0201

8c. ADDRESS (City, State, and ZIP Code)	10 SOURCE OF FUNDING NUMBERS			
	PROGRAM ELEMENT NO.	PROJECT NO.	TASK NO	WORK UNIT ACCESSION NO

11. TITLE (Include Security Classification) Electrochemistry and Spectroelectrochemistry of 1,8-Napthalene and 1,8-Anthracene-Linked Cofacial Binuclear Metallophthalocyanines. New Mixed Valence Metallophthalocyanines.

12 PERSONAL AUTHOR(S) N. Kobayashi, H. Lam, W.A. Nevin, P. Janda, C.C. Leznoff and A.B.P. Lever

13a. TYPE OF REPORT Technical	13b. TIME COVERED FROM Aug. '89 TO Aug. '90	14 DATE OF REPORT (Year, Month, Day) May 10, 1990	15. PAGE COUNT 53

16. SUPPLEMENTARY NOTATION

17	COSATI CODES		18. SUBJECT TERMS (Continue on reverse if necessary and identify by block number)
FIELD	GROUP	SUB-GROUP	Phthalocyanine, Binuclear, Perchlorinated, Cofacial, Mixed Valence, film, polymers ad (# G)

19 ABSTRACT (Continue on reverse if necessary and identify by block number) Cobalt

1,8-Napthalene or 1,8-anthracene-linked cofacial dizinc, dicopper, and dicobalt diphthalocyanines have been studied by solution and surface electrochemistry, spectroelectrochemistry, and electron spin resonance (ESR). These derivatives are mixtures of syn and anti isomers which have very similar electrochemistry except where we comment specifically. The phthalocyanine ring first oxidation Pc(-1)/Pc(-2), the Co(III)/Co(II) and Co(II)/Co(I) redox couples split into two couples as a consequence of intra-ring exchange interactions. The spectra of the electrochemically oxidised or reduced species, and in particular, those of the mixed valence species are recorded. Exciton coupling energies are derived and are seen to be related to the ground state mixed valence splitting energies. These are discussed in terms of structure and inter-ring distance. Cobalt derivatives immobilized onto ordinary pyrolytic graphite catalyze the electroreduction of oxygen by two electrons to hydrogen peroxide.

20. DISTRIBUTION / AVAILABILITY OF ABSTRACT ☒ UNCLASSIFIED/UNLIMITED ☐ SAME AS RPT ☐ DTIC USERS	21. ABSTRACT SECURITY CLASSIFICATION Unclassified/unlimited
22a. NAME OF RESPONSIBLE INDIVIDUAL Dr. Robert K. Grasselli	22b. TELEPHONE (Include Area Code) 22c. OFFICE SYMBOL

DD FORM 1473, 34 MAR

83 APR edition may be used until exhausted
All other editions are obsolete

SECURITY CLASSIFICATION OF THIS PAGE

TECHNICAL REPORT DISTRIBUTION LIST, GENERAL

	No. Copies		No. Copies
Office of Naval Research Chemistry Division, Code 1113 800 North Quincy Street Arlington, VA 22217-5000	3	Dr. Ronald L. Atkins Chemistry Division (Code 385) Naval Weapons Center China Lake, CA 93555-6001	1
Commanding Officer Naval Weapons Support Center Attn: Dr. Bernard E. Douda Crane, IN 47522-5050	1	Chief of Naval Research Special Assistant for Marine Corps Matters Code 00MC 800 North Quincy Street Arlington, VA 22217-5000	1
Dr. Richard W. Drisko Naval Civil Engineering Laboratory Code L52 Port Hueneme, California 93043	1	Dr. Bernadette Eichinger Naval Ship Systems Engineering Station Code 053	1
Defense Technical Information Center Building 5, Cameron Station Alexandria, Virginia 22314	2 high quality	Philadelphia Naval Base Philadelphia, PA 19112	
David Taylor Research Center Dr. Eugene C. Fischer Annapolis, MD 21402-5067	1	Dr. Sachio Yamamoto Naval Ocean Systems Center Code 52 San Diego, CA 92152-5000	1
Dr. James S. Murday Chemistry Division, Code 6100 Naval Research Laboratory Washington, D.C. 20375-5000	1	David Taylor Research Center Dr. Harold H. Singerman Annapolis, MD 21402-5067 ATTN: Code 283	1

ONR Electrochemical Sciences Program
Abstracts Distribution List (9/89)

Dr. Henry White
Department of Chemical Engineering and
Materials Science
421 Washington Ave., SE
Minneapolis, MN 55455
(612) 625-3043
400o027yip

Dr. A. B. P. Lever
Department of Chemistry
York University
4700 Keele Street
North York, Ontario M3J 1P3
(416) 736-2100 Ext. 2309
4131025

Dr. Mark Wrighton
Department of Chemistry
Massachusetts Institute of Technology
Cambridge, MA 02139
(617) 253-1597
4131027

Dr. Michael Weaver
Department of Chemistry
Purdue University
West Lafayette, IN 49707
(317) 494-5466
4133001

Dr. Lesser Blum
Department of Physics
University of Puerto Rico
Rio Piedras, PUERTO RICO 00931
(809) 763-3390
4133002

Dr. R. David Rauh
EIC Laboratories, Inc.
111 Downey Street
Norwood, MA 02062
(617) 769-9450
4133003

Dr. Rudolph Marcus
Division of Chemistry and Chemical Engineering
California Institute of Technology
Pasadena, CA 91125
(818) 356-6566
4133004

Dr. Donald Sandstrom
Boeing Aerospace Company
P.O. Box 3999, M/S 87-08
Seattle, WA 98124-2499
(206) 773-2272
4133007

Dr. Ernest Yeager
Director, Case Center for
Electrochemical Sciences
Case Western Reserve University
Cleveland, OH 44106
(216) 368-3626
4133008

Dr. B. S. Pons
Department of Chemistry
University of Utah
Salt Lake City, UT 84112
(801) 581 4760
4133010

Dr. Michael R. Philpott
IBM Research Division
Almaden Research Center
650 Harry Road
San Jose, CA 95120-6099
(408) 927-2410
4133011

Dr. Ulrich Stimming
Department of Chemical Engineering
and Applied Chemistry
Columbia University
New York, NY 10027
(212) 280-8755
4133014

Dr. Royce W. Murray
Department of Chemistry
University of North Carolina at Chapel Hill
Chapel Hill, NC 27514
(919) 962-6295
4133015

Dr. Daniel Buttry
Department of Chemistry
University of Wyoming
Laramie, WY 82071
(307) 766-6677
4133019

Dr. Joseph Hupp
Department of Chemistry
Northwestern University
Evanston, IL 60208
(312) 491-3504
4133025

Dr. Martin Fleischmann
Department of Chemistry
The University
Southampton SO9 5NH
UNITED KINGDOM
0703-559122
4134001

Dr. Joel Harris
Department of Chemistry
University of Utah
Salt Lake City, UT 84112
(801) 581-3585
413a005

Dr. Gregory Farrington
Laboratory for Research on the
Structure of Matter
3231 Walnut Street
Philadelphia, PA 19104-6202
(215) 898-6642
413d003

Dr. D. E. Irish
Department of Chemistry
University of Waterloo
Waterloo, Ontario, CANADA N21 3G1
(519) 885-1211 ext. 2500
4133016

Dr. W. R. Fawcett
Department of Chemistry
University of California, Davis
Davis, CA 95616
(916) 752-1105
4133020

Dr. Andrew Ewing
Department of Chemistry
152 Davey Laboratory
Pennsylvania State University
University Park, PA 16802
(814) 863-4653
4133030

Dr. Allen Bard
Department of Chemistry
The University of Texas at Austin
Austin, TX 78712-1167
(512) 471-3761
413a002

Dr. J. O. Thomas
Institute of Chemistry, Box 531
University of Uppsala
S-751 21 Uppsala
SWEDEN
413d003

Dr. Charles Martin
Department of Chemistry
Texas A&M University
College Station, TX 77843
(409) 845-7638
413d005

Dr. C. A. Angell
Arizona State University
Department of Chemistry
Tempe, AZ 85287
(602) 965-7217
413d007

Dr. Martha Greenblatt
Department of Chemistry
Rutgers University
Piscataway, NJ 08854
(201) 932-3277
413d008

Dr. Bruce Dunn
Departement of Materials Science and
Engineering
University of California, Los Angeles
Los Angeles, CA 90024
(213) 825-1519
413d011

Dr. James Brophy
Department of Physics
University of Utah
Salt Lake City, UT 84112
(801) 581-7236
413d015

Dr. Richard Pollard
Department of Chemical Engineering
University of Houston, University Park
4800 Calhoun, Houston, TX 77004
(713) 749-2414
413d016

Dr. Nathan S. Lewis
Division of Chemistry and Chemical Engineering
California Institute of Technology
Pasadena, CA 91125
(415) 723-4574
413d017

Dr. Hector Abruña
Department of Chemistry
Cornell University
Ithaca, NY 14853
(607) 256-4720
413d018

Dr. Adam Heller
Department of Chemical Engineering
The University of Texas at Austin
Austin, TX 78712-1062
(512) 471-5238
413h007

Dr. Petr Vanýsek
Department of Chemistry
Northern Illinois University
Dekalb, IL 60115
(815) 753-6876
413k001

Dr. George Wilson
Department of Chemistry
University of Kansas
Lawrence, KS 66045
(913) 864-4673
413k002

Dr. H. Gilbert Smith
EG&G Mason Research Institute
57 Union Street
Worcester, MA 01608
(617) 791-0931
413k003

Electrochemistry and Spectroelectrochemistry of 1,8-Naphthalene and

1,8-Anthracene-Linked Cofacial Binuclear Metallophthalocyanines. New Mixed Valence

Metallophthalocyanines

Nagao Kobayashi,[*][1] Herman Lam, W. Andrew Nevin,[2] Pavel Janda,[3] Clifford C.

Leznoff,[*] and A. B. P. Lever.[*]

Department of Chemistry, York University, North York (Toronto), Ontario, Canada M3J

1P3

1,8-Naphthalene or 1,8-anthracene-linked cofacial dizinc, dicopper, and

dicobalt diphthalocyanines have been studied by solution and surface

electrochemistry, spectroelectrochemistry, and electron spin resonance (ESR).

These derivatives are mixtures of _syn_ and _anti_ isomers which have very similar

electrochemistry except where we comment specifically. The phthalocyanine

ring first oxidation Pc(-1)/Pc(-2), the Co(III)/Co(II) and Co(II)/Co(I) redox

couples split into two couples as a consequence of intra-ring exchange

interactions. The spectra of the electrochemically oxidised or reduced

species, and in particular, those of the mixed valence species are recorded.

Exciton coupling energies are derived and are seen to be related to the ground

state mixed valence splitting energies. These are discussed in terms of

structure and inter-ring distance. Cobalt derivatives immobilized onto

ordinary pyrolytic graphite catalyze the electroreduction of oxygen by two

electrons to hydrogen peroxide.

Introduction

There is considerable interest in the electrochemistry and spectroelectrochemistry of binuclear metalloporphyrins[4-7] and binuclear[8-10] and polynuclear[8d,8e,9,10] metallophthalocyanines. When two macrocyclic units are spaced closely to each other, properties which are not seen in mononuclear units often emerge. Most striking of these is the splitting of some redox couples, generating mixed-valence species whose properties have been discussed for several systems.[4,6,7c,8a,b,e,10] Mixed valence behaviour has been observed with some zinc derivatives of flexible clamshell phthalocyanines[8e], but not with analogous cobalt derivatives.

We report the electrochemical and spectroelectrochemical properties of rigidly linked 1,8-naphthalene and 1,8-anthracene bridged cofacial binuclear metallophthalocyanines (Fig. 1), to explore their exchange interactions and capacity for mixed valence species formation. As shown below, interactions in the pillared phthalocyanines are larger than in corresponding porphyrins, and the formation of mixed-valence redox states is observed. In contrast to the flexible clamshell species, cobalt complexes of these pillared species do exhibit mixed valence behaviour both at the cobalt atom, and at the phthalocyanine ring. This is the first detailed study of the mixed valence behaviour of transition metal metallophthalocyanine species.

In addition, we describe the catalytic behaviour of the cobalt derivatives for the electroreduction of oxygen, since several cofacial cobalt porphyrins are known to function as excellent catalysts for this reaction.[11,12]

While phthalocyanines have traditionally been important to the pigment, paint and ink industry, they are also now employed as the photoconductive layer in photocopying equipment. Moreover their unusual chemical stability coupled with their intense colour and redox activity is leading to considerable worldwide interest in developing more high technology applications. These include

electrochromic devices, chemical sensors, molecular metals, laser dyes, optical disks, photovoltaic cells, fuel cells etc., as well as applications in medicine, such as photodynamic cancer therapy.[13] Mixed valence species are likely to be of value in some of these applications and thus such studies have both fundamental and potential industrial benefit over a wide field.

Experimental Section

The synthesis, purification, and characterization of the naphthalene[8a,14] (Nap[MTrNPc]₂) and anthracene (Ant[MTrNPc]₂) linked[14] binuclear phthalocyanines and mononuclear metallotetraneopentoxy phthalocyanines[15] (MTNPcs) are described elsewhere. N,N-dimethyl formamide (DMF) (Aldrich, Gold label, anhydrous, H_2O <0.005% packed under nitrogen), and o-dichlorobenzene (DCB) (Aldrich, Gold label) were used as supplied. Tetrabutylammonium perchlorate (TBAP)(Kodak) was recrystallized from absolute ethanol and dried at 50 °C under vacuum for 2 days.

Electronic spectra were recorded with a Perkin-Elmer Hitachi Model 340 microprocessor spectrometer. Cyclic and differential pulse voltammetry were performed with a Princeton Applied Research (PARC) 174A Polarographic Analyzer coupled to a PARC 175 Universal programmer. Electrochemical data were recorded under an atmosphere of nitrogen, or argon, using a conventional three electrode cell. A platinum disk described by the cross-sectional area of a 27-gauge wire (area 10^{-3} cm²), sealed in glass, was used as the working electrode, a platinum wire served as the counter electrode, and the reference electrode was Ag/AgCl (-0.045 V vs. SCE)[16] (in sat. KCl, separated by a frit) corrected for junction potentials by being referenced internally to the ferrocenium/ferrocene (Fc⁺/Fc) couple. In various experiments involving DMF solutions, the Fc⁺/Fc couple was seen to lie in the range +0.35 to +0.45 V vs. Ag/AgCl/Cl⁻, due to variations in junction potentials. In DCB, the Fc⁺/Fc couple was observed at approximately 0.59 V vs. Ag/AgCl/Cl⁻.[17]

All DMF solutions were prepared and measurements were made under an atmosphere

of nitrogen within a Vacuum Atmospheres Drilab. The DCB solutions were prepared in air, degassed by repeated freeze-pump-thaw cycles, and then transferred to the drybox. The stability of the Ag/AgCl/Cl⁻ electrode was checked using a solution of ferrocene in DCB; it was stable for at least two days. Spectroelectrochemical measurements were made with a 0.45 mm pathlength optically transparent thin layer electrode (OTTLE) cell, utilyzing a gold minigrid (500 lines/in., 60% transmittance),[18] or with a 1 mm pathlength OTTLE utilizing a Pt minigrid,[19] in conjunction with the Hitachi Perkin-Elmer spectrometer.

Potential scans for oxygen reduction were performed with a Pine Instrument RD3 potentiostat and the rotating studies with a Pine Instrument PIR rotator. The working electrode material for oxygen reduction studies is ordinary pyrolytic graphite (OPG) and has a circular area of 0.44 cm^2. Before each experiment, the OPG electrode surface was cleaned by successive polishings with 1.0, 0.3, and 0.005 μm alumina (Linde) suspended in water on a Metron polishing cloth. For the adsorption of the catalysts onto the OPG surface, the electrode was immersed in ca. 1-5 x 10^{-5} M phthalocyanine solution for ca. 10 minutes, removed from the solution and washed with ethanol and distilled water and dried under reduced pressure. Judging from the cyclic voltammetric curve under argon at the prepared electrode, the surface concentration of the catalyst becomes steady-state by an immersion of less than 10 minutes. The cell comprised a separate chamber for each electrode, with a Luggin capillary extending from the reference chamber to the proximity of the OPG surface. For the aqueous experiments, a saturated calomel electrode (SCE) and a large platinum plate were used as a reference and a counter electrode, respectively. Argon gas (Linde) was purified by passage through heated copper filings, anhydrous $CaSO_4$ (Drierite), molecular sieves (BDH 3A), and glass wool. Oxygen gas (Linde) was purified by passage through anhydrous $CaSO_4$, NaOH pellets (AnalaR), molecular sieves, and glass wool.

Solutions for electrochemistry and spectroelectrochemistry contained 0.1-0.3 M

TBAP, as supporting electrolyte.

Electron spin resonance (ESR) data were obtained using a Varian E4 spectrometer, calibrated with diphenylpicrylhydrazide (DPPH). ESR spectra of electrochemically generated Nap[CoTrNPc]$_2$ species in the presence or absence of 2-methyl imidazole were obtained by bulk electrolysis of a solution (degassed by freeze-pump-thaw cycles) under an atmosphere of nitrogen in the dry box, and transferring the species to sealable ESR tubes. Control electronic spectra were also taken. The bulk electrolysis cell consisted of a platinum plate working electrode, a Pt flag counter electrode, and a silver wire quasi-reference electrode. Counter and reference electrodes were separated from the working compartment by medium glass frits.

Results and Discussion

Complex NMR absorptions of Nap[H$_2$TrNPc]$_2$ in the region of δ =7.3-8.5 have been analyzed as an approximately 1:1 mixture of syn and anti isomers[8a,14] in the metal-free derivative. It is likely that all the metal complexes are also mixtures of syn and anti isomers, but the proportions may vary from 1:1. Each of the syn and anti isomers of Nap or Ant[MTrNPc]$_2$ exists as a mixture of 36 regioisomers with respect to the neopentoxy substituent. Previous studies[8] of such regioisomer mixtures have indicated that they have essentially identical electrochemical and optical properties and are largely inseparable by chromatographic methods. The properties of the syn and anti isomers are, however, expected to be different, as further developed below.

(i) **Electron Spin Resonance.** Two Cu(II)(I=3/2) ions in close proximity frequently produce two strong perpendicular transitions which may result in seven equally spaced lines in the g=2 region of their ESR spectra.[20,21] The ESR spectrum of Nap[CuTrNPc]$_2$ shows (Fig. 2A) a peak and a trough at g=2.192 and 1.902, due to two perpendicular transitions by two equivalent and coupled Cu(II) ions in addition to a signal due to uncoupled Cu(II) ions (g= 2.025). A seven-line pattern did not

appear. The mixed spectra obtained here stem from the presence of the _syn_ and _anti_ isomers which affect the Cu-Cu bond distance and are important to this analysis.

Accordingly, the signals at $g=2.192$ and 1.902 are associated with the _syn_ isomer, while the $g=2.025$ signal is due to the _anti_ isomer. It is impossible to evaluate the Cu-Cu distance from this spectrum, since the zero field splitting parameters are not obtainable. However, judging from the X-ray crystallographic data on 1,8-diphenylnaphthalene whose two phenyl groups are forced apart from each other, the Cu-Cu distance in the _syn_ form of this compound should be at least 4.3 Å. If CPK molecular models are used for this purpose, a rather larger value would result.[22,23]

The ESR spectra of the $Nap[CoTrNPc]_2$ species were recorded in DCB at 77 K. In the absence of an axial ligand, the ESR spectra of both $Nap[Co(II)TrNPc]_2$ and its one-electron reduced $[Co(II)TrNPc.Co(I)TrNPc]^-$ species exibited no signal. When 2-methylimidazole was added to the one electron reduced species, however, an ESR spectrum typical of a cobalt(II) center axially coordinated by a nitrogeneous base[11c] was obtained (Fig. 2B), although its shape was slightly deformed ($g=2.25$). Unfortunately, a clear hyperfine splitting of the parallel component which would provide a clue as to whether a cobalt nucleus ($I=7/2$) is interacting with a nitrogen nucleus ($I=1$) or with another cobalt nucleus, was not observed. The cause may be the presence of _syn_ and _anti_ isomers. We will show below that the one-electron reduced species is a $Nap[Co(II)TrNPc][Co(I)TrNPc]^-$ mixed valence compound.

(ii) **Electrochemistry.** In general, in the electrochemical data which follow, we describe either simultaneous two-electron processes where oxidation or reduction of the binuclear molecule occurs at the same potential in both rings, or step-wise oxidations or reductions where mixed valence species are generated by the sequential redox of each ring. Note that the simultaneous two-electron processes will have the characteristics of a one-electron process, but with twice the

current.[16] Further, the assignment of mixed valence products may not always be
unequivocally determined by the electrochemical data in the sense that additional
waves could conceivably have arisen from impurity or decomposition products.
However all the mixed valence species have been characterised by
spectro-electrochemistry, described below, and thus the electrochemical assignments
are secure.

(a) <u>Zinc and Copper Derivatives</u>. Fig. 3 shows typical cyclic and/or differential
pulse voltammograms (CV and DPV respectively) of ZnTNPc and Ant[ZnTrNPc]$_2$ in DMF or
DCB. Data on mononuclear ZnTNPc,[8s] are shown here for comparison. Redox
assignments are based on this mononuclear ZnTNPc control data (Table I).
Ant[ZnTrNPc]$_2$ gave two oxidation and two reduction couples in DMF, corresponding in
potential to two <u>quasi</u>-reversible one-electron reductions and one <u>quasi</u>-reversible
one-electron oxidation of the phthalocyanine ring ($i_a = i_c$, $i \propto \underline{v}^{1/2}$). From the
amount of current in the cyclic voltammogram and/or the area of the peaks in the
DPV voltammogram, the two reduction waves involve two electrons each, per binuclear
molecule, while the two oxidation couples are associated with approximately one
electron each, per binuclear molecule.

Similar behaviour has been reported for a flexible zinc phthalocyanine
binuclear molecule linked by a five-atom bridge, EtMeO(5)[ZnTrNPc]$_2$,[8s] where
EtMeO(5) represents an ($-OCH_2 C(Me)(Et)CH_2 O-$) bridge. In that case, controlled
potential electrochemistry confirmed that the first and second oxidation waves
arose through the stepwise oxidation of the two phthalocyanine rings,[8s] i.e.
Pc(-2)Pc(-2) ---> Pc(-2)Pc(-1) ---> Pc(-1)Pc(-1).[24] The two oxidation waves
observed with Ant[ZnTrNPc]$_2$, are similarly assigned since oxidation to the doubly
oxidized Pc(-0) level lies at a much more positive potential.[8c-s] Ring oxidation of
the monomeric species lies at a potential lying between the two ring oxidation
potentials of the cobalt and zinc binuclear species. Similar behaviour is observed
in the binuclear μ-oxo bridged silicon phthalocyanine,[9c] compared with the

mononuclear species.

In DCB, all the redox couples of ZnTNPc (Fig. 3A (c)) and Ant[ZnTrNPc]₂ (Fig. 3B (c)) lie negative of those in DMF. However as in DMF, the first ring oxidation of two phthalocyanine units in Ant[ZnTrNPc]₂ in DCB proceeded in a stepwise fashion, with potential separation _ca._ 210 mV compared with 150mV for EtMeO(5)[TrNPcZn]₂ (Tables I, II).[8a] The reduction couples of Ant[ZnTrNPc]₂, in DCB, look much more irreversible than in DMF and spectroelectrochemistry (vide infra), could not be used because of species instability. Probably, the first two reduction couples involve the stepwise reduction of two phthalocyanine rings but the data are not of sufficient quality to warrant detailed discussion. Nap[ZnTrNPc]₂ behaves essentially similarly to Ant[ZnTrNPc]₂.

The cyclic and differential voltammetric behaviour of Nap[CuTrNPc]₂ in comparison to CuTNPc is similar to that of Nap[ZnTrNPc]₂ or Ant[ZnTrNPc]₂ to ZnTNPc in DCB. However, low solubility in DMF hindered determination of some of the redox couples even by DPV. In DCB, Nap[CuTrNPc]₂ exhibited two _quasi_-reversible and one irreversible oxidation and two _quasi_-reversible reductions (Table I). An additional less intense peak appeared between the first and second reductions, in both solvents. Compared with Nap[ZnTrNPc]₂, the potential difference (1.65 V) between the first oxidation and reduction couples is larger by 0.24 V, while that (0.31 V) between the first and second reductions is smaller by 0.11 V. Possibly the two reduction steps are stepwise one-electron reductions processes via a mixed valence reduction species, but solubility problems prevent their elucidation. Fig. 4A shows a stick diagram comparison of the relevant mononuclear and binuclear species couples.

(b) Cobalt Derivatives.   Voltammograms of the cobalt complexes differ from the zinc and copper complexes in showing redox couples due to metal oxidation and reduction. Within the limit of solvent breakdown, in DCB (Fig. 5), CoTNPc shows five redox couples which have been previously assigned[8c] (as indicated in curve A).

Nap[CoTrNPc]$_2$ and Ant[CoTrNPc]$_2$ displayed a pair of overlapping couples around 0 V,

whose total charge corresponds to two electrons, per binuclear molecule, (curves B

and C). These couples are assigned to phthalocyanine ring oxidation, based upon

spectroelectrochemical data (next section).

The position of this composite couple is approximately the same as that of the

first phthalocyanine ring oxidation in Nap[CuTrNPc]$_2$, Nap[ZnTrNPc]$_2$, and

Ant[ZnTrNPc]$_2$, the splitting of the two component bands being a little smaller:

moreover the DPV peak to the positive side appears to be larger than the other. The

reduction corresponding to the Co(II)/Co(I) couple of CoTNPc, in DCB, shows at

least two couples, the more positive DPV wave again being larger in appearance than

the other. However since the second reduction step shows some irreversibility (most

clearly seen in the cyclic voltammograms), the relative currents in the DP

voltammograms may not indicate simple concentration ratios.

Variations in relative DPV heights may also reflect different kinetic

parameters for the redox processes involving the syn and anti isomers. The

Co(II)/Co(I) splitting in the syn isomer should be somewhat greater than that of

the anti isomer. Since the forward and reverse DPVs shown in Figs.5,6 are

essentially the same, it is possible that the electrochemical data may reflect a

larger relative concentration of syn rather than anti isomer in the binuclear metal

complexes under consideration. The anti isomer, even though involving longer

cobalt-cobalt distances than the syn isomer, is expected to show some mixed valence

splitting since it differs from the earlier studied clamshell binuclear species[8c],

in being inflexible (see below). In the zinc species discussed above, the

contributions from the two isomers are not distinguished but these also show

greater current in the more positive component of the split waves. Note that these

variations in current for components of a given couple do not occur in the

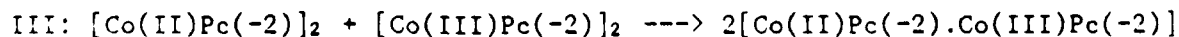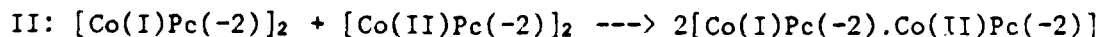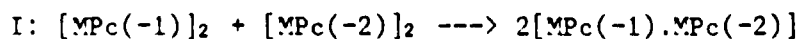EtMeO(5)[ZnTrNPc]$_2$ and zinc tetramer redox processes.[8a]

The splitting of the two bands is ca. 480 mV for Ant[CoTrNPc]$_2$ and 390 mV for

Nap[CoTrNPc]₂ in DCB, about twice as large as the splitting of the phthalocyanine

ring oxidation couples (Tables II and III). Although not clear in the case of

Nap[CoTrNPc]₂, another small but explicit redox couple is discerned for

Ant[CoTrNPc]₂ at ca. -0.9 V vs Fc⁺/Fc (curve B); this may be the first reduction

couple for the <u>anti</u> isomer. We return to this discussion below

(spectroelectrochemistry).

In DMF,[8c] CoTNPc shows Co(II)/Co(I) and Co(III)/Co(II) couples before the

reduction and oxidation respectively of the ligand (see also Fig. 6A). The

corresponding couples in Ant[CoTrNPc]₂ and Nap[CoTrNPc]₂ are split, and the area of

each peak in the DPV voltammogram (see Fig. 6B for Ant[CoTrNPc]₂) roughly

corresponds to one electron, per binuclear molecule (Table III).

In both DCB and DMF, the first reduction of the two phthalocyanine rings

occurs simultaneously at the same potential around -2 V. Compared with the first

ring reduction of dizinc and dicopper derivatives, the potential is roughly 500 mV

more negative, a consequence of the central Co(I) metal ion, compared with central

Zn(II) and Cu(II) metal ions in the former species.[8f] This Co(I)Pc(-2)/Co(I)Pc(-3)

anion radical reduction wave is unsplit and occurs at essentially the same

potential in the mononuclear CoTNPc and, evidently, both the <u>syn</u> and <u>anti</u> isomers

of the Nap and Ant binuclear species. This must be a net two-electron reduction

process (per binuclear molecule) in the latter species.

(iii) <u>Comproportionation Constants</u>. In order to obtain information about the

stability of mixed valence species, comproportionation constants (K_c at 20 °C) of

the mixed valence formation reactions were calculated, using eqn.(1) (Table II),

I: [MPc(-1)]₂ + [MPc(-2)]₂ ---> 2[MPc(-1).MPc(-2)]

II: [Co(I)Pc(-2)]₂ + [Co(II)Pc(-2)]₂ ---> 2[Co(I)Pc(-2).Co(II)Pc(-2)]

III: [Co(II)Pc(-2)]₂ + [Co(III)Pc(-2)]₂ ---> 2[Co(II)Pc(-2).Co(III)Pc(-2)]

and

$$\Delta E = (RT/F)\ln K_c \qquad\qquad (1)$$

where ΔE is the splitting energy for the relevant split redox couple. The K_c values lie approximately in the $1 \times 10^3 - 3 \times 10^8$ range (ΔG = ca. -17---> -49 kJ mol^{-1}), indicative of significant delocalization in many of the complexes.[27]. Table II contains a comparison of literature data for related processes (see (viii) below for further comment).

(iv) <u>Electronic Spectra</u>. The rigid geometry of the naphthalene or anthracene bridge induces important changes in these cofacial metal derivatives, compared with mononuclear phthalocyanines.[8c]. The divalent metal M(II)Pc(-2) species all show a doubled Q band (Table IV, Figs. 7,8 and Fig. 1a of ref[8a]) indicative of exciton interaction between the two halves of the molecule.[28,29] The situation is complicated by the presence of both the <u>syn</u> and <u>anti</u> isomers but the higher energy component can securely be assigned to the allowed Q band, exciton split, component of the <u>syn</u> isomer. The lower energy absorption then arises from overlap of <u>anti</u> isomer absorption and weaker "forbidden" <u>syn</u> isomer absorption.

Assuming no ground state interaction betweeen the π levels of the phthalocyanine rings, the exciton splitting in the <u>syn</u> isomer may be estimated as twice the difference between the higher energy component in the Q band absorption of the binuclear species, and the Q band observed in the mononuclear MTNPc control molecules[8c,8a] in the solvent concerned (Table IV). In this fashion the so-called "uncorrected" data in Table V are derived. Exciton coupling is also estimated, qualitatively, from the ratio of the peak intensities of the upper energy Q component to that of the lower energy. The greater the degree of coupling between the two halves of the molecule, the greater will be the intensity of the higher energy component; such data are also reported in Table V.

However the existence of mixed valence ring-oxidation species is a direct indication of a ground state interaction between the phthalocyanine π levels. Indeed the extent of electrochemical splitting, ΔE of the pair of oxidation levels

is _inversely_ proportional to the "uncorrected" exciton energies (cf. Tables II and V). This is contrary to the intuitive expectation that the greater the ground state interaction, the greater the degree of exciton coupling.

A qualitative molecular orbital description might be written as in Fig. 9. To the extent that the ground state π levels interact as in Fig. 9, the Q band transition will be red shifted, nominally by the energy y (in Fig. 9), relative to the mononuclear species. The quantity y is related to ΔE (for ring oxidation) and it is relevant that the higher energy Q band component does shift to _lower_ energy with increasing ΔE. This provides evidence that this simple qualitative model, which has also been used to describe the properties of silicon phthalocyanine dimers and trimers,[10] has merit, and explains the apparent inverse dependence mentioned immediately above.

The quantity y may be approximated as the difference in energy between the first oxidation potential of the control mononuclear MTNPc species, and the more negative of the split components of the oxidation of the binuclear species. The values of y are also shown in Table V and do generally increase with increasing (ring oxidation) splitting energy ΔE. The "corrected" exciton splitting is then approximately equal to the "uncorrected" value plus $2y$. These data are also reported in Table V.

Although the "corrected" exciton coupling energies are subject to some uncertainty, an increase in exciton splitting does parallel an increase in electrochemical (ring oxidation) splitting, ΔE, of the ground state for these, and related, binuclear cobalt and zinc species (Tables III and V).

Q band half-bandwidths are also listed in Tables, II,V. They are a complex function since the Q band, normally of half-bandwidth around 300-800 cm^{-1}, will broaden as a consequence of some exchange coupling. However, in the limit of coupling between two phthalocyanine rings where the binuclear species is strictly of D_{4h} symmetry, the bandwidth becomes narrower due to loss of the lower energy

transition which becomes forbidden.[29] For example, the highly cofacial crown ether phthalocyanine binuclear species have half-bandwidths of the order of 700-1000 cm^{-1}.[21] The rather larger values reported here in Table V reflect the presence of the _anti_ isomer, and the relatively low symmetry of the cofacial _syn_ isomer. The narrowness of the Q band for the Nap[ZnTrNPc]$_2$ species in DMF is, however, noteworthy.

Comparison of the band envelopes of the anthracene and naphthalene cobalt(II) species, with the clamshell species (Fig. 5 of ref.[8c]) show that the latter have slightly greater absorption in the long wavelength tail, even though the half-bandwidths (ca 2700-2800 cm^{-1}) are essentially the same. The lack of a long wavelength tail in the Q band region of the naphthalene and anthracene species suggests that they conform more closely to D$_{4h}$ symmetry than do the flexible clamshell species.

(v) _Spectroelectrochemistry_ To assign the redox couples and to observe the interaction between the halves of the molecules, as a function of oxidation state, spectroelectrochemical experiments were performed for Ant[CoTrNPc]$_2$ and Nap[CoTrNPc]$_2$ in optically transparent thin layer electrode (OTTLE) cells. Data for the naphthalene species have been previously briefly described (Fig. 1 of ref.[8a]). Fig. 7 shows the absorption spectra of Ant[CoTrNPc]$_2$ in DCB. In a similar manner to reduction of the Nap[CoTrNPc]$_2$ species,[8a] reduction across the first couple results in the spectroscopic changes shown in A, with isosbestic points occurring at 562, 648, and 765 nm, and a change of colour from blue to green.

In common with Co(I)Pc species, a new absorption band appears in the region of 400-500 nm, associated with metal-to-ligand charge-transfer (MLCT) from cobalt(I) to the phthalocyanine ring;[30] there is also an increase in intensity in the Soret region. The Q-band spectrum of this green solution and that of the corresponding Nap[CoTrNPc]$_2$ reduced species are unlike any seen previously for reduced cobalt phthalocyanines,[19,30] having a strong Q band at ca. 660 nm instead of the usual

band at 710 nm. This is similar, however, to the mixed valence flexible clamshell
EtMeO(5)[ZnPc(-2).ZnPc(-1)]$^+$ species described earlier.[8s]

The second reduction between -1.3 and -1.8 V (Fig. 7B) gives a yellow
solution, with isosbestic points at 329, 395, 570, 683, and 762 nm. The final
spectrum is very similar to that of the mononuclear Co(I)TNPc species,[8c] thus both
cobalt atoms have been reduced to Co(I). The reduced (Co(I).Co(I)) species is
fully reversible to the starting material by oxidation positive of the first
reduction couple on the spectroelectrochemical time scale (minutes) even though the
2nd reduction step is irreversible.

Nernstian plots of the spectroelectrochemical data over each of the reduction
processes give slopes of 55 and 48 mV (for the first and second reduction,
respectively, of Nap[CoTrNPc]$_2$ in DCB), and intercepts of -0.29 and -0.64V vs
AgCl/Ag respectively; thus each step involves a one-electron transfer and the
product of the first reduction must be a mixed valence species of mainly
[Co(II)TrNPc.Co(I)TrNPc]$^-$ character. Taking the Fc$^+$/Fc couple to be about 0.59V vs
AgCl/Ag gives intercept values of -0.88 and -1.23V vs Fc$^+$/Fc, which are close to
the values measured by CV (Table III).

For the mixed valence [Co(II)TrNPc.Co(I)TrNPc]$^-$ species (Fig. 7A) the
intensity of the MLCT band appears to be only about 20% of that of the fully
reduced [Co(I)TrNPc.Co(I)TrNPc]$^{2-}$ species. This may signify that at the potential
employed to obtain this electronic spectrum, only the _syn_ isomer is reduced fully
to Co(II).Co(I) while the _anti_ isomer, which would be reduced at a somewhat more
negative potential is only partially reduced to Co(II).Co(I). Given the overlapping
nature of the Q band spectra of the Co(II).Co(II) and Co(II).Co(I) species, the
spectrum shown in Fig. 7A for the mixed valence species might well contain some
unreduced _anti_ species.

The presence of the well-resolved Q band at 660 nm, rather than 710 nm
indicates some coupling between the formal Co(II) and Co(I) halves of the molecule.

A weak absorption band of the first reduction product in the region of 800-900 nm (Fig. 7A) may be an intervalence band. Nap[CoTrNPc]2 also shows similar spectroscopic changes in the corresponding processes.[8a] The positions of the Q band peaks of the first and second reduction products, however, are shifted by about 10 nm to shorter wavelength compared with Ant[CoTrNPc]2.

The similarity in the final spectrum of the [Co(I)TrNPc.Co(I)TrNPc]$^{2-}$ species to that of mononuclear [Co(I)TNPc]$^-$ requires that there is little interaction between the two halves of the binuclear molecule in the [Co(I)TrNPc.Co(I)TrNPc]$^{2-}$ species. Each half will carry a net negative charge and this may force them slightly further apart than in the [Co(II)TrNPc.Co(II)TrNPc] or [Co(II)TrNPc.Co(I)TrNPc]$^-$ species. Evidently both the <u>syn</u> and <u>anti</u> forms of the [Co(I)TrNPc(-2).Co(I)TrNPc(-2)]$^{2-}$ species must have very similar spectra. Similar behaviour is observed in DMF solution.

Fig. 8A demonstrates spectroscopic changes of Ant[CoTrNPc]2 in DCB observed during stepwise oxidation. As seen in Fig. 5B, the first oxidation couples are composed of a superimposition of two couples. Changes in Fig. 8A also contain two processes. In the oxidation between -0.4 and -0.1 V, the absorbance of a peak at 635 nm decreases but that at 670 nm increases, while in the second oxidation at potentials higher than 0 V, the absorbance in the whole Q band region decreases. During these oxidations, the absorbance at ca. 340-570 nm increases. In the oxidation of phthalocyanines, the increase of absorbance in the region between the Soret and the Q bands is an indication of phthalocyanine ring oxidations,[8c,e,31,32]; therefore the first oxidation of Ant[CoTrNPc]2 in DCB forms the cobalt(II) phthalocyanine cation radical species.

Fig. 8B shows the spectroscopic changes of Ant[CoTrNPc]2 in DMF observed during the first oxidation. As the potential is increased through the region of the two oxidation waves a peak at 630 nm decreases but that at 660 nm develops into an intense peak at 673 nm. During this process, no new peak appears between the Soret

and the Q bands. This behaviour is typical for the oxidation of cobalt(II) to

cobalt(III) phthalocyanine.[8c,d,30d,e,33]

The spectroscopic development in Fig. 8B corresponds to the process from the

[Co(II)TrNPc.Co(II)TrNPc] to the fully oxidised Ant[Co(III)TrNPc]$_2^{2+}$ species with

no distinct intermediate spectrum attributable to a mixed valence

[Co(III)TrNPc.Co(II)TrNPc]$^+$ species being observed. Such a species must certainly

exist. However the Q band energy maxima for Co(II)TNPc and Co(III)TNPc are

essentially identical[8c]. Thus in the absence of a strong perturbing interaction

between the two halves of the mixed valence species, its spectroscopic signature

will be difficult to discern. Indeed the inability to see this intermediate leads

one to exclude a strong spectroscopic perturbation for this mixed valence species.

(vi) Immobilization of Nap and Ant[CoTrNPc]$_2$ on OPG. Argon data

Fig. 10. shows the cyclic voltammograms at Nap[CoTrNPc]$_2$ adsorbed on OPG in

deaerated 0.05 M H$_2$SO$_4$ solution. A redox couple with equal reduction and oxidation

current is seen at ca. -0.28 V vs. SCE. The potential of this couple shifts with

changing pH of the solution as demonstrated in Fig. 11, shifting negatively with

increasing pH between pH 1 and 7 with a slope of -(60-70) mV/pH unit; above ca. pH

9 it becomes essentially pH independent. Similar behaviour has been found in

several cobalt phthalocyanine systems,[34] and the relevant couple is ascribed to

that of Co(II)/Co(I).

Assuming the wave corresponds to a Faradaic change in the charge of the

adsorbed species by nF, and the system behaves ideally, the ratio of the slope of a

plot of peak current vs. sweep rate to the charge should be equal to nF/4RT, where

n is the number of electrons per adsorbed species and the other symbols have their

usual meaning.[35] Experimental values give unexpectedly lower values of

(0.5-0.6)F/RT compared with those of (0.8-0.9)F/RT for a mononuclear control

molecule, CoTNPc.[34a] Such low values have been observed previously for immobilized

cofacial porphyrins,[4f] and attributed to the presence of inactive material on the

surface. In the case of the porphyrin, the surface concentration was derived from consideration of how much material was laid upon the electrode surface. In this case using the slope analysis, any inactive material will neither contribute to q nor n, and the calculation is therefore unresponsive to the presence of inactive material on the surface, except insofar as this may have kinetic significance. Indeed the simple analysis described here would only be valid for pure Nernstian behaviour and fast kinetics.[16] It is possible that the deviation from 1 electron per cobalt atom is attributable to kinetic interference in the electron transfer. Nevertheless it is interesting that it is the adsorbed binuclear phthalocyanine species, and not the mononuclear species, which give rise to this reduced value of n.

This wave is therefore the first reduction wave to the mixed valence Nap[Co(II)TrNPc.Co(I)TrNPc]$^-$ species on the surface. The second reduction wave should be seen some 0.2 - 0.5 V more negative; however proton reduction to hydrogen is catalysed by cobalt phthalocyanine[36] and occurs some 0.15 - 0.20V more negative than the first wave, thereby obscuring this second wave. Moving to higher pH does not alleviate the problem since proton reduction tracks the pH behaviour of this first couple. No advantage was found in switching to stress annealed pyrolytic graphite as support material. Thus the second reduction wave cannot be identified.

(vii) Electrocatalytic reduction of oxygen: When the solution in Fig. 10A is saturated with oxygen, the responses shown in Fig. 10B are obtained. In cyclic voltammograms, a cathodic peak appears at -0.20 V vs. SCE whose current (i_p) is proportional to the concentration of oxygen and the square root of the scan rate, indicating that this i_p is controlled by the diffusion of oxygen. Compared with the Co(II)/Co(I) redox couple of this catalyst, the catalytic O_2 reduction wave appears at a more positive potential at all pHs.

Using standard rotating disk electrode (RDE) methods[34b,35,37,38] two-electron reduction of oxygen to hydrogen peroxide is observed. A rotating ring-disk

electrode experiment (not shown) detected hydrogen peroxide at the ring electrode upon reduction of oxygen at the disk electrode. Similar electrochemical behaviour is also observed at Ant[CoTrNPc]$_2$ modified electrodes. Thus, in contrast to some cofacial bis(cobalt) porphyrins[11,12] which catalyze O_2 reduction by a four-electron pathway to water at pH less than 2, Nap and Ant[CoTrNPc]$_2$ catalyze O_2 reduction only to hydrogen peroxide in the pH range 1-14.

In considering the mechanism of O_2 reduction, it is clear at least that cobalt is participating in the reaction, since the O_2 reduction peak potential tracks the Co(II)/Co(I) redox potential at all pHs; however the mechanism is unclear. Although the potential difference between the Co(II)/Co(I) couples and O_2 reduction peak is a little over 200 mV in alkaline solution, an EC mechanism is possible if the reaction rate is very fast.[39] The potential difference of 200 mV, for example, corresponds to a reaction rate of ca. 5×10^8 $M^{-1}s^{-1}$ which is an order of magnitude larger than for some porphyrin[38,40] and phthalocyanine[19] systems. This problem has been discussed in depth elsewhere, where an alternate mechanism involving binding of oxygen to cobalt(II) phthalocyanine is presented.[34b]

(viii) Concluding Comments.

The electrochemical behavior of the cofacial phthalocyanine binuclear molecules in this paper, is similar to that of the cofacial porphyrins.[4-7] In these complexes, splitting of both the Co(II)/Co(I) and Co(III)/Co(II) redox couples has been observed and appears a function of the nature of the inter-ring linkage. Co(II).Co(I) splitting energies of some 0.25 - 0.4V are observed, perhaps a little smaller than the largest observed here. Curiously for the 1,8-anthracene linked cofacial dicobalt diporphyrin (Ant[CoPor]$_2$)[4a] which has a similar structure to Ant[CoTrNPc]$_2$, there is no observable splitting of the Co(II)/Co(I) wave, and no dramatic change in electronic spectrum. Metallophthalocyanines[41] are more planar than porphyrins,[42] and, perhaps because of this property, have a much higher tendency towards cofacial aggregation than porphyrins.[43] The approach of the two

phthalocyanine units in one naphthalene or anthracene binuclear species, may be closer therefore, than in the corresponding binuclear porphyrin.

Table II summarises the splitting energies observed for a range of phthalocyanine species. Although, several factors affect the size of K_c,[27a] electrostatic interactions must play an important role. Particularly in the syn form, the two phthalocyanine planes are in close proximity. However the distance between the phthalocyanine units in the 1,8-naphthalene species has been estimated as at least 4.3 Å (section i), compared with the van der Waals contact (3.6 Å)(or shorter in some silicon bridged phthalocyanine species, 3.3 Å).[9c,10] The mixed valence splitting energies for oxidation of the silicon phthalocyanine RSiPc-O-PcSiR binuclear species are of the order of 0.4-0.5V[10] and therefore rather larger than those reported here. This value is indicative of that to be expected at close contact when the rings are well aligned.

The mixed valence splitting energies for reduction of the silicon binuclear species are about 0.4V,[10] and likely provide an upper limit for sideways interactions of the τ clouds in the reduced ring species.   This splitting is comparable or less than the Co(II).Co(I) splitting data reported here. These larger Co(II).Co(I) values are likely a consequence of the interaction between the cobalt d_{z^2} orbitals which point directly towards one another along the inter-ring axis. While magnetic studies could provide useful information concerning the electronic structures of both the [Co(II)TrNPc.Co(II)TrNPc] and [Co(II)TrNPc.Co(I)TrNPc]$^{-1}$ series of complexes, it is premature to attempt such measurements until a means has been found to separate the syn and anti isomers.

Comparison of the "corrected" exciton data (Table V) of these anthracene and naphthalene species with the flexible clamshell EtMeO(5) species, does show that the former have greater exciton splitting and this is consistent with the increased electrochemical mixed valence splitting.

The lack of mixed valence oxidation products for the cobalt flexible clamshell

species may reflect the formation of six coordinate Co(III) species when a donor solvent or electrolyte anion is present, thus forcing the two rings apart. This may also occur with Co(II)Pc(-1) species since formation of the Pc(-1) oxidation state will increase the Lewis acidity of the cobalt atom.

Stepwise oxidation of the two rings in a binuclear phthalocyanine species places a positive charge on one ring, which will then attract the electron density on the other ring, favouring formation of a mixed valence delocalised oxidation species. On the other hand, there is no firm evidence for the formation of mixed valence anion radical species in the current series of binuclear complexes, albeit that the DCB electrochemical data are ambiguous in this respect. In this redox level there is an added electron making one ring negatively charged and causing repulsion of the other ring.

Thus mixed valence behaviour has been established for the following classes of phthalocyanine compound:-

Pc(-1).Pc(-2)- Observed with cobalt, and in main group species such as silicon and zinc. Although not fully investigated here it is likely that mixed valence Pc(-1).Pc(-2) species containing either cobalt(II) or cobalt(III) can be derived by appropriate choice of solvent or medium.

Co(II).Co(I) - Observed in inflexible binuclear cobalt phthalocyanines, this mixed valence species has significant stability due to delocalisation of the charge.

Co(III).Co(II)- Observed in inflexible binuclear phthalocyanines.

Pc(-2).Pc(-3)- Observed in rigid main group M-bridge-M species such as RSiPc-O-PcSR, but less readily obtained in flexible binuclear species.

There is every reason to expect that the above observations are fairly general and that most transition metal ions would yield mixed valence complexes in pillared

phthalocyanine species. This study provides the foundation for future studies in mixed valence phthalocyanine chemistry. It is possible to predict with some certainly the situations which should give rise to mixed valence phthalocyanine chemistry, and estimate the energetics thereof and hence to use this capability in a design sense for technological application.

Bibliography and Notes

(1) Visiting Professor from the Pharmaceutical Institute, Tohoku University,
     Sendai 980, Japan.

(2) Current address: Central Research Laboratories, Kanegafuchi Chemical Industry
     Co. Ltd., 2-80, 1-Chome, Yoshida-cho, Hyogo-ku, Kobe 652, Japan.

(3) Visiting research associate from the Heyrovsky Institute of the Czech Academy
     of Sciences, Prague, Czechoslovakia.

(4) (a) Mest, Y. L.; L'Her, M.; Collman, J. P.; Kim, K.; Helm, S.; Hendricks, N.
     H. J. Electroanal. Chem. 1987, 234, 277; 1987, 220, 247. (b) Collman, J. P.;
     Prodolliet, W.; Leidner, R. J. Am. Chem. Soc. 1986, 108, 2916. (c) Le Mest,
     Y.; Courtot-Coupez, J.; Collman, J. P.; Evitt, E. R.; Bencosme, C. S. J.
     Electroanal. Chem. 1985, 184, 331. (d) Collman, J. P.; Marrocco, M.; Elliot,
     C. M.; L'Her, M. L. ibid., 1981, 124, 113. (e) Collman, J. P.; Kim, K.;
     Leidner, C, R. Inorg. Chem. 1987, 26, 1152; f) Ngameni, E.; Le Mest, Y.;
     L'Her, M.; Collman, J.P.; Hendricks, N.H.; Kim, K. J.Electroanal.Chem. 1987,
     220, 247.

(5) Cowan, J. A.; Saunders, J. K. M. J. Chem. Soc., Perkin Trans.I 1987, 2395.

(6) (a) Crossley, M. J.; Burn, P. L. J. Chem. Soc., Chem. Commun. 1987, 39. (b)
     Buchler, J. W.; Elsasser, K. Angew. Chem. Int. Ed. Engl. 1986, 25, 286. (c)
     Williams, R. F. X.; White, D.; Hambright, P.; Schamin, A.; Little, R. G. J.
     Electroanal. Chem. 1983, 110, 69. (d) Becker, J. Y.; Dolphin, D.; Paine, J. B.
     Wijesekera, T. J. ibid., 1984, 164, 335.

(7) Bottomley, L. A.; Gorce, J. -N.; Landrum, J. T. Inorg. Chim. Acta 1986, 125,
     135. (b) Kadish, K. M.; Cheng, J. S.; Cohen, I. A.; Summerville, D. ACS
     Symposium Ser. 1977, No. 38, 65. (c) Kadish, K. M.; Larson, G.; Lexa, D.;
     Momenteau, M. J. Am. Chem. Soc. 1975, 97, 282.

(8) (a) Leznoff, C. C.; Lam, H.; Nevin, W. A.; Kobayashi, N.; Janda, P.; Lever, A.
     B. P. Angew. Chem. Int. Ed. Engl. 1987, 26, 1021. (b) Leznoff, C. C.;Lam, H.;

Marcuccio, S. M.; Nevin, W. A.; Janda, P.; Kobayashi, N.; Lever, A. B. P. _J._ _Chem. Soc., Chem. Commun._ 1987, 699. (c) Nevin, W. A.; Hempstead, M. R.; Liu, W.; Leznoff, C. C.; Lever, A. B. P. _Inorg. Chem._, 1987, _26_, 570. (d) Nevin, W. A.; Liu, W.; Greenberg, S.; Hempstead, M. R.; Marcuccio, S. M.; Melnik, M.; Leznoff, C. C.; Lever, A. B. P. _Inorg. Chem._ 1987, _26_, 891. (e) Liu, W.; Hempstead, M. R.; Nevin, W. A.; Melnik, M.; Lever, A. B. P.; Leznoff, C. C. _J._ _Chem. Soc., Dalton Trans_. 1987, 2511. (f) Minor, P. C.; Lever, A. B. P. _Inorg._ _Chem._ 1983, _22_, 826. (g) Manivannan, V.; Nevin, W. A.; Leznoff, C. C.; Lever, A. B. P. _J. Coord. Chem._ 1988, _19_, 139. (h) Leznoff, C. C.; Greenberg, S.; Marcuccio, S. M.; Minor, P. C.; Seymour, P.; Lever, A. B. P.; Tomer, K. B. _Inorg. Chim. Acta_ 1984, _89_, L35.

(9)   (a) Simic-Glavaski, B.; Tanaka, A. A.; Kenney, M. E.; Yeager, E.; _J._ _Electroanal. Chem._ 1987, _229_, 285. (b) Mezza, T. M.; Armstrong, N. R.; Kenney, M. J. _Electroanal. Chem._ 1984, _176_, 259. (c) Mezza, T. M.; Armstrong, N. R.; Ritter, G. W.; Iafalice, J. P.; Kenney, M. E. _J. Electroanal. Chem_. 1982, _137_, 227.

(10) Wheeler, B. L.; Nagasubramanian, G.; Bard, A. J.; Schechtman, L. A.; Dininny, D. R.; Kenney, M. E. _J. Am. Chem. Soc_. 1984, _106_, 7404. Anderson, A. B.; Gordon, T. L.; Kenney, M. E. _J. Am. Chem. Soc_. 1985, _107_, 192; DeWulf, D.W.; Leland, J.K.; Wheeler, B.L.; Bard, A.J.; Batzel, D.A.; Dininny, D.R.; Kenney, M.E. _Inorg.Chem._, 1987, _26_, 266.

(11) (a) Collman, J. P.; Marrocco, M.; Denicevich, P.; Koval, C.; Anson, F. C. _J._ _Electroanal. Chem._ 1979, _101_, 117; _J. Am. Chem. Soc_, 1980, _102_, 6027. (b) Durand, R. R.; Bencosme, C. S.; Collman, J. P.; Anson, F. C. _J. Am. Chem. Soc_. 1983, _105_, 2694, 2710. (c) Collman, J. P.; Anson, F. C.; Bencosme, C. S.; Durand, R. R.; Kreh, R. P. _J. Am. Chem. Soc_. 1983, _105_, 2699.

(12) (a) Liu, H. Y.; Weaver, M. J.; Wang, C. B.; Chang, C. K. _J. Electroanal. Chem_. 1983, _145_, 439. (b) Chang, C. K.; Liu, H. Y.; Abdalmuhdi, I. _J. Am. Chem. Soc_.

1984, 106, 2725. (c) Ni, C. -L.; Abdalmuhdi, I.; Chang, C. K.; Anson, F. C. J. Phys. Chem. 1987, 91, 1158. (d) Liu, H. Y.; Abdalmuhdi, I.; Chang, C. K.; Anson, F. C. J. Phys. Chem. 1985, 89, 665.

(13) Lever, A.B.P. Chemtech, 1987, 17, 506-10; The Phthalocyanines; Leznoff, C.C; Lever, A.B.P. Eds.; VCH: New York, 1989.

(14) Lam, H.; Marcuccio, S.M.; Svirskaya, P.I.; Greenberg, S.; Lever, A. B. P.; Leznoff, C. C.; Zerny, C. Can. J. Chem. 1989, 67, 1087.

(15) Leznoff, C. C.; Marcuccio, S. M.; Greenberg, S.; Lever, A. B. P.; Tomer, K. B. Can. J. Chem. 1985, 63, 623.

(16) Bard, A. J.; Faulkner, L. R. "Electrochemical Methods," John Wiley, New York, 1980.

(17) The position of the ferrocenium/ferrocene couple is quite sensitive to the organic solvent employed. Gagne, R. R.; Koval, C. A.; Lisensky, D. C. Inorg. Chem. 1980, 19, 2854; Gritzner, G.; Kuta, J. Electrochim. Acta 1984, 29, 869; Bohling, D.A.; Evans, J.F.; Mann, K.R. Inorg.Chem., 1982, 21, 3546.; Bagchi, R.N.; Bond, A.M.; Colton, R.; Luscombe, D.L.; Moir, J.E. J.Am.Chem.Soc., 1986, 108, 3352; Harman, W.D.; Sekine, M.; Taube, H. J.Am.Chem.Soc., 1988, 110, 5725.

(18) Nevin, W. A.; Lever, A. B. P. Anal.Chem. 1988, 60, 727.

(19) Kobayashi, N.; Nishiyama, Y. J. Phys. Chem. 1985, 89, 1167.

(20) Chikira, M.; Yokoi, H.; Isobe, T. Bull. Chem. Soc. Jpn. 1974, 47, 2208.; Chikira, M.; Kon, H.; Hawley, R. A.; Smith, K. M. J. Chem. Soc., Dalton Trans. 1979, 246 and some refs. cited therein. Chasteen, N. D.; Belford, R. L. Inorg. Chem. 1970, 9, 169.

(21) Kobayashi, N.; Lever, A. B. P. J. Am. Chem. Soc. 1987, 109, 7433.

(22) This Cu-Cu distance is considerably larger than the distance between the 1 and 8 positions of naphthalene (ca.2.5 Å).[23a] The CPK model also suggests that the two phthalocyanine planes are stretching apart from each other, because the 1

and 8 positions of naphthalene are too close for them to be attached. In the

1,8-anthracene linked diphthalocyanine series, such a phenomenon should not

take place. Accordingly, the Cu-Cu distance in the _syn_ isomer is considered to

be approximately equal to the distance between the 1 and 8 positions of

anthracene (ca. 4.95 Å).[23b]

(23) (a) House, H. O.; Koepsell, D. G.; Campbell, W. J. _J. Org. Chem_. 1972, _37_,

1003. (b) Fillers, J. P.; Ravichandran, K. G.; Abdalmuhdi, I.; Chang, C. K. _J._

Am. Chem. Soc. 1986, _108_, 417.

(24) The standard oxidation state of the phthalocyanine anion is represented by

Pc(-2). Thus the first oxidised and first reduced species will be represented

by Pc(-1) and Pc(-3) respectively, see:- Myers, J. F.; Rayner, J. W.; Lever,

A. B. P. _Inorg. Chem_. 1975, _14_, 461.

(25) Walker, F. A. _J. Am. Chem. Soc._ 1973, _95_, 1150, 1154; Stynes, D. V.; Stynes,

H. C.; James, B. R.; Ibers, J. A. _ibid_. 1973, _95_, 1796; James, B. R. "The

Porphyrins", Vol. V, Dolphin, D. Ed.; Academic Press: New York, 1978; pp

258-277.

(26) Minor, P.C., Ph.D. Thesis, York University, 1983.

(27) (a) Gagne, R. R.; Spiro, C. L.; Smith, T. J.; Haman, C. A.; Thies, W. R.;

Shiemke, A. K. _J. Am. Chem. Soc_. 1981, _103_, 4073. (b) Sutton, J. E.; Taube, H.

Inorg. Chem. 1981, _20_, 319. (c) Suzuki, M.; Uehara, A.; Oshio, H.; Yanaga, M.;

Kida, S.; Sato, K. _Bull. Chem. Soc. Jpn_. 1987, _60_, 3547.

(28) Kasha, M.; Rawls, H. R.; Et-Bayoumi, M. A. _Pure Appl. Chem_. 1965, _11_, 371.

(29) Dodsworth, E. S.; Lever, A. B. P.; Seymour, P.; Leznoff, C. C. _J. Phys. Chem_.

1985, _89_, 5698.

(30) (a) Nevin, W. A.; Liu, W.; Melnik, M.; Lever, A. B. P. _J. Electroanal. Chem_.

1986, _213_, 217; (b) Rollman, L. D.; Iwamoto, R. T. _J.Am. Chem. Soc_. 1968, _90_,

1455; (c) Clack, D. W.; Yandle, J. R. _Inorg. Chem_. 1972, _11_, 1738; (d) Day,

P.; Hill, H. A. O.; Price, M. G. _J. Chem. Soc. A_ 1968, 90; (e) Stillman, M.

J.; Thompson, A. J. <u>J. Chem. Soc., Faraday Trans.2</u> 1974, <u>70</u>, 790; (f) Le

Moigne, J.; Even, R. J. <u>J. Chem. Phys</u>. 1985, <u>82</u>, 6472; (g) Taube, R. <u>Z. Chem</u>.

1966, <u>6</u>, 8; h) Lever, A. B. P.; Licoccia, S.; Magnell, K.; Minor, P. C.;

Ramaswamy, B. S. <u>ACS Symp. Ser</u>, 1982, <u>No.201</u>, 237;

(31) Minor, P. C.; Gouterman, M.; Lever, A. B. P. <u>Inorg. Chem</u>. 1985, <u>24</u>, 1894.

(32) (a) Dolphin, D.; James, B. R.; Murray, A. J.; Thornback, J. R. <u>Can. J. Chem</u>.
1980, <u>58</u>, 1125; (b) Ferraudi, G.; Oishi, S.; Muraldiharan, S. <u>J. Phys. Chem</u>.
1984, <u>88</u>, 5261; (c) Nyokong, T.; Gasyna, Z.; Stillman, M. J. <u>Inorg. Chim. Acta</u>
1986, <u>112</u>, 11; (d) Gavrilov, V.; Tomilova, L. G.; Shelepin, I. V.; Luk'yanets,
E. A. <u>Elektrokhimiya</u> 1979, <u>15</u>, 1058.

(33) Homborg, H.; Kalz, W. <u>Z. Naturfolsch., B.; Anorg. Chem., Org. Chem</u>. 1984, <u>39B</u>,
1490; Kalz, W.; Homborg, H.; Kuppers, H.; Kennedy, B. J.; Murray, K. S. <u>ibid</u>.
1984, <u>39B</u>, 1478.

(34) (a) Zecevic, S.; Simic-Glavaski, B.; Yeager, E.; Lever, A. B. P.; Minor, P. C.
<u>J. Electroanal. Chem</u>. 1985, <u>196</u>, 339. (b) Janda, P.; Kobayashi, N.; Auburn, P.
R.; Lam, H.; Leznoff, C. C.; Lever, A. B. P. <u>Can. J. Chem</u>. 1989, <u>67</u>, 1109.

(35) Zagal, J.; Bindra, P.; Yeager, E. <u>J. Electroanal. Chem</u>. 1977, <u>83</u>, 207.

(36) Bernstein, P.; Lever, A.B.P. Paper in preparation.

(37) (a) Durand, R. R.; Anson, F. C. <u>J. Electroanal. Chem</u>. 1982, <u>134</u>, 273. (b)
Shigehara, K.; Anson, F. C. <u>J. Phys. Chem</u>. 1982, <u>86</u>, 2776.

(38) (a) Forshey, P. A.; Kuwana, T. <u>Inorg. Chem</u>. 1981, <u>20</u>, 693; 1983, <u>22</u>, 699. (b)
Forshey, P. A.; Kuwana, T.; Kobayashi, N.; Osa, T. <u>Adv. Chem. Ser</u>. 1982, <u>No.</u>
<u>201</u>, 601.

(39) (a) Oyama, N.; Oki, N.; Ohno, H.; Ohnuki, Y.; Matsuda, H.; Tsuchida, E. <u>J.</u>
<u>Phys. Chem</u>. 1983, <u>87</u>, 3642. (b) Andrieux, C. P.; Saveant, J. M. <u>J.</u>
<u>Electroanal. Chem</u>. 1982, <u>134</u>, 163; 1982, <u>142</u>, 1. (c) Andrieux, C. P.;
Dumas-Bouchiat, J. M.; Saveant, J. M. <u>ibid</u>. 1982, <u>131</u>, 1.

(40) (a) Kobayashi, N.; Fujihira, M.; Osa, T.; Kuwana, T. <u>Bull. Chem. Soc. Jpn</u>.

1980, <u>53</u>, 2195. (b) Kobayashi, N.; Osa, T. <u>J. Electroanal. Chem</u>. **1983**, <u>157</u>, 269. (c) Ozer, P.; Parash, R.; Broitman, F.; Mor, U.; Bettelheim, A. <u>J. Chem. Soc., Faraday Trans. I</u> **1984**, <u>80</u>, 1139.

(41) Robertson, J. M.; Woodward,I. <u>J. Chem. Soc</u>. **1937**, 219.

(42) (a) Hoard, J. L. In "<u>Porphyrins and Metalloporphyrins</u>"; Smith, K. M., Ed.; Elsevier: Amsterdam, New York, Oxford, 1975; Chap. 8. (b) Scheidt, W. R. In "<u>The Porphyrins</u>" Dolphin, D. Ed.; Academic Press: New York, London, 1978; Vol. III, Chap. 10.

(43) (a) Ref.3 in ref. 21. (b) White, W. I. In "<u>The Porphyrins</u>" Dolphin, D. Ed.; Academic Press: New York, London, 1978; Vol. V, Chap.7.

Figure Captions

Figure 1. Naphthalene and anthracene-linked cofacial binuclear
metallophthalocyanines used in the present study. "Syn" structures are shown.

Figure 2. ESR spectra of (A) Nap[CuTrNPc]$_2$ in toluene and (B)
Nap[Co(II)TrNPc(-2)][Co(I)TrNPc(-2)]$^-$ in the presence of 2-methyl imidazole in
DCB at 77 K. [Nap[CuTrNPc]$_2$]/M = 1 x 10^{-3}. [Nap [CoTrNPc]$_2$]/M = 2.6 x 10^{-4}.
[2-methylimidazole]/M = 2 x 10^{-3}. In (B), solution contains 0.13 M TBAP.

Figure 3. Cyclic and differential pulse voltammograms of (A) ZnTNPc and (B)
Ant[ZnTrNPc]$_2$ in DMF (curves a and b) and in DCB (curves c) at Pt-disk working
electrode. Scan rates/mV s^{-1} = 100 for cyclic voltammetry and 5 for
differential pulse (DP) voltammetry. In DP diagrams, solid lines indicate
cathodic scan and dotted lines anodic scan. [ZnTNPc]/M = ca. 1 x 10^{-3} in DMF
and 3 x 10^{-3} in DCB. [Ant[ZnTrNPc]$_2$]/M = ca. 4 x 10^{-4} in DMF and 2.64 x 10^{-4}
in DCB. [TBAP]/M = 0.3.

Figure 4. Schematic stick representation of redox couple potentials in MTNPc, and
the anthracene and naphthalene species, A) for Zinc, and B) for Cobalt.

Figure 5. Cyclic and differential pulse (DP) voltammograms of (A) CoTNPc, (B)
Ant[CoTrNPc]$_2$, and (C) Nap[CoTrNPc]$_2$ in DCB at a Pt disk working electrode.
Scan rates/mV s^{-1} = 50, 100, and 200 for cyclic voltammetry and 5 for DPV
voltammetry. In DPV diagramms, solid lines indicate cathodic scan and dotted
lines anodic scan. [CoTNPc]/M = 6 x 10^{-4}, [Ant[CoTrNPc]$_2$]/M = 3 x 10^{-4},
[Nap[CoTrNPc]$_2$]/M = 3.6 x 10^{-4}, and [TBAP]/M = 0.3. Assignments of redox
couples are shown for CoTNPc from the literature.[8c]

Figure 6. Cyclic and DPV voltammograms of (A) CoTNPc and (B) Ant [CoTrNPc]$_2$ in DMF
at Pt-disk working electrode. Numbers indicate scan rates in mV s^{-1}. In the
DPV diagrams, the solid line and dotted line, respectively, indicate cathodic
and anodic scans. [CoTNPc]/M = ca. 7.1 x 10^{-4}, [Ant[CoTrNPc]$_2$]/M = ca. 3.8 x
10^{-4}, and [TBAP]/M = 0.3. Assignments of redox couples are shown for CoTNPc

from the literature.[8c]

Figure 7.   Development of the electronic spectra of Ant[CoTrNPc]₂ in DCB with time,

showing the formation of (A) the mixed valence [Co(II)TrNPc.Co(I)TrNPc]⁻

species, and (B) the doubly reduced [Co(I)TrNPc.Co(I)TrNPc]²⁻ species obtained

by reduction at potentials between −0.8 and −1.2 V, and −1.3 and −1.6 V,

respectively. [Ant[CoTrNPc]₂]/M = 1.17 x 10⁻⁴. [TBAP]/M = 0.3. Pathlength/mm

= 0.45.

Figure 8.   Development of the electronic spectra of Ant[CoTrNPc]₂ in (A) DCB or in

(B) DMF, showing the formation of (A) Ant[Co(II)TrNPc(-2).Co(II)TrNPc(-1)]⁺

and then Ant[Co(II)TrNPc(-1)]₂²⁺ species, and (B) the doubly oxidized

Ant[Co(III)TrNPc(-2)]₂²⁺ species obtained by oxidation at potentials between

−0.5 and +0.6 V. Pathlength/mm = 0.45. [Ant[CoTrNPc]₂]/M = 1.27 x 10⁻⁴ in

DCB and 2.05 x 10⁻⁴ in DMF. [TBAP]/M = 0.3.

Figure 9. A molecular orbital description of the interaction between the τ and τ^*

levels of a pair of interacting cofacial phthalocyanine rings. The arrows

indicate allowed transitions, while the hatched lines indicate forbidden

transitions in D_{4h} symmetry. The allowed transitions are of approximately the

same energy and correspond with the observed high energy component of the Q

band in the binuclear species. The energy y corresponds approximately with

the difference in first oxidation potential of the mononuclear and binuclear

species. In this model, the u---->u transition becoming slightly allowed in

reduced symmetry acentric species provides the long wavelength tail of the Q

band absorption.

Figure 10. Cyclic voltammograms (solid lines) and RRDE response (broken line) at

Nap[CoTrNPc]₂ adsorbed on OPG electrode in the (A) absence and (B) presence of

oxygen in 0.05 M H₂SO₄. In (A), the dotted line indicates response at a bare

OPG electrode. Numbers in the figure indicate scan rate in mV s⁻¹.

Figure 11. pH Dependence of the Co(II)/Co(I) redox potential of CoTNPc,

Nap[CoTrNPc]$_2$, and Ant[CoTrNPc]$_2$ adsorbed onto OPG, and that of the O$_2$

reduction potential at these phthalocyanine adsorbed electrodes. In oxygen

reduction, peak potentials (CV method) or half-way potentials (RRDE method)

are plotted.

Table I Electrochemical Data for Mononuclear and Binuclear Zinc and Copper Derivatives

----

	DCB Solution		DMF Solution	
System/Couple	$E_{1/2}/V^a$	$\triangle E_p/mV^b$	$E_{1/2}/V^a$	$\triangle E_p/mV^b$

ZnTNPc				
Pc(0)/Pc(-1)	0.64[c,d]			
Pc(-1)/Pc(-2)	-0.02	120	0.05[e]	85
Pc(-2)/Pc(-3)	-1.66	110	-1.43	95
Pc(-3)/Pc(-4)	-2.04	65	-1.85	95
Ant[ZnTrNPc]$_2$				
[Pc(-1)]$_2$/[Pc(-1).Pc(-2)]	0.08	(70)	0.16	(85)
[Pc(-1).Pc(-2)]/[Pc(-2)]$_2$	-0.13	(80)	-0.05	(75)
[Pc(-2)]$_2$/[Pc(-2).Pc(-3)]	-1.54[f]	100		
[Pc(-2)]$_2$/[Pc(-3)]$_2$			-1.41	70
[Pc(-2).Pc(-3)]/[Pc(-3)]$_2$	-1.80[g]	110		
[Pc(-3)]$_2$/[Pc(-4)]$_2$			-1.93	60
Nap[ZnTrNPc]$_2$				
[Pc(0)]$_2$/[Pc(-1)]$_2$?	0.73[f]		0.71[g]	80
[Pc(-1)]$_2$/[Pc(-1).Pc(-2)]	0.07	(50)	0.19	(80)
[Pc(-1).Pc(-2)]/[Pc(-2)]$_2$	-0.14	(50)	0.01	(70)
[Pc(-2)]$_2$/[Pc(-3)]$_2$	-1.67, -1.83[d]	(70)	-1.47	100
[Pc(-3)]$_2$/[Pc(-4)]$_2$	-2.02[d]	110	-1.85	70

Nap[CuTrNPc]$_2$[h]

[Pc(0)]$_2$/[Pc(-1)]$_2$?	0.74[e]			
[Pc(-1)]$_2$/[Pc(-1).Pc(-2)]	0.27	(50)	0.41[d]	
[Pc(-1).Pc(-2)]/[Pc(-2)]$_2$	0.07	(50)	0.11[d]	
[Pc(-2)]$_2$/[Pc(-3)]$_2$	-1.58	60	-1.28	50
[Pc(-3)]$_2$/[Pc(-4)]$_2$	-1.89	80	-1.72	60

----

a) Potentials are reported with respect to the ferrocenium/ferrocene couple. $E_{1/2}$

values were measured by cyclic voltammetry at 200, 100, 50 and 20 mV/s. Average

data being $E = (E_{pa} + E_{pc})/2$ are reported. Data in parenthesis are estimated

from overlapping waves. b) Values of $\triangle E_p = (E_{pa} - E_{pc})$ are given at a potential

sweep rate of 50 mV/s. c) data fom ref.8g. d) Potentials are approximate because

the waves are weak or broad. Reported values of $E_{1/2}$ were obtained by

differential pulse voltammetry. e) The position of this wave shifts to higher

potential in more concentrated solutions. These data were collected in solutions

of approximately 10^{-4} M.

f) Assignment of these couples is tentative. Because of instability at high

potentials, spectroelectrochemistry could not be performed to confirm these

assignments. g) Irreversible couple. h) This compound displayed a weak extra

couple at -1.75 and -1.52V in DCB or DMF respectively.
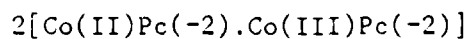
Table II Comproportionation Data

Couple[a]	Solvent[b]	E(V)[c]	K_c[d]	K_d[e]	$\triangle G/kJmol^{-1}$
Ant[CoTrNPc]$_2$	I	DCB	0.17	8.4×10^2	1.2×10^{-3}	-17
	II	DCB	0.48	1.8×10^8	5.6×10^{-9}	-47
	III	DMF	0.23	9.0×10^3	1.1×10^{-4}	-23
	II	DMF	0.30	1.4×10^5	7.0×10^{-6}	-29.5
Nap[CoTrNPc]$_2$	I	DCB	0.14	2.8×10^2	2.5×10^{-3}	-14
	II	DCB	0.39	4.0×10^6	2.5×10^{-7}	-38
	III	DMF	0.24	1.3×10^4	7.5×10^{-5}	-24
	II	DMF	0.22	6.1×10^3	1.65×10^{-4}	-22
EtMeO(5)(ZnPc)$_2$[f]	I	DCB	0.08	2.4×10^1	4.2×10^{-2}	-8
	I	DMF	0.15	3.8×10^2	2.6×10^{-3}	-15
(ZnTrNPc)$_4$[f]	I	DCB	0.11	7.8×10^1	1.3×10^{-2}	-11
	I	DMF	0.15	3.8×10^2	2.6×10^{-3}	-15
Ant[ZnTrNPc]$_2$	I	DCB	0.21	4.1×10^3	2.45×10^{-4}	-21
	I	DMF	0.21	4.1×10^3	2.45×10^{-4}	-21
Nap[ZnTrNPc]$_2$	I	DCB	0.21	4.1×10^3	2.45×10^{-4}	-21
	I	DMF	0.18	1.2×10^3	8.0×10^{-4}	-18
Nap[CuTrNPc]$_2$	I	DCB	0.20	2.7×10^3	3.6×10^{-4}	-20
(-1)(ZnPc)$_2$[g]	I	DCB	0.26	2.95×10^4	3.4×10^{-5}	-25
	I	DMF	0.22	6.1×10^3	1.65×10^{-4}	-22
RSiPc-O-PcSiR[h]	I	CH$_2$Cl$_2$	0.49	2.7×10^8	3.7×10^{-9}	-49
	II	CH$_2$Cl$_2$	0.40	7.6×10^6	1.3×10^{-7}	-40

a) I: $[MPc(-1)]_2 + [MPc(-2)]_2 \longrightarrow 2[MPc(-1).MPc(-2)]$

II: $[Co(I)Pc(-2)]_2 + [Co(II)Pc(-2)]_2 \longrightarrow 2[Co(I)Pc(-2).Co(II)Pc(-2)]$

III: $[Co(II)Pc(-2)]_2$ + $[Co(III)Pc(-2)]_2$ --->

$$2[Co(II)Pc(-2).Co(III)Pc(-2)]$$

For the cobalt complexes, data refer to the _syn_ isomer. b) Solvent DMF = dimethylformamide, DCB = o-dichlorobenzene. c) mixed valence splitting energy. d) Comproportionation constant. e) Disproportionation constant, $1/K_c$. f) ref.8g. g) ref 34d h) R = $n-C_6H_{13}$, ref 10.

Table III Electrochemical Data for Mononuclear and Binuclear Cobalt Derivatives

System/Couple	DCB Solution		DMF Solution	
	$E_{1/2}/V^a$	$\triangle E_p/mV^b$	$E_{1/2}/V^a$	$\triangle E_p/mV^b$
CoTNPc				
$Co^{III}Pc(0)/Co^{III}Pc(-1)$	0.87	140		
$Co^{III}Pc(-1)/Co^{II}Pc(-1)$	0.59	190		
$Co^{III}Pc(-1)/Co^{III}Pc(-2)$	----------		0.38	80
$Co^{II}Pc(-1)/Co^{II}Pc(-2)$	0.03	125		
$Co^{III}Pc(-2)/Co^{II}Pc(-2)$	----------		-0.02	75
$Co^{II}Pc(-2)/Co^{I}Pc(-2)$	-0.91	210	-0.85	120
$Co^{I}Pc(-2)/Co^{I}Pc(-3)$	-2.07	145	-1.99	85
Ant[CoTrNPc]₂				
$[Co^{III}Pc(-2)]_2/[Co^{III}Pc(-2).Co^{II}Pc(-2)]$	----------		0.22	50
$[Co^{II}Pc(-1)]_2/[Co^{II}Pc(-1).Co^{II}Pc(-2)]$	0.06	80	----------	
$[Co^{III}Pc(-2).Co^{II}Pc(-2)]/[Co^{II}Pc(-2)]_2$	----------		-0.01	70
$[Co^{II}Pc(-1).Co^{II}Pc(-2)]/[Co^{II}Pc(-2)]_2$	-0.11	40	----------	
$[Co^{II}Pc(-2)]_2/[Co^{II}Pc(-2).Co^{I}Pc(-2)]$	-0.78	55	-0.73	90
	-0.91	30		
$[Co^{I}Pc(-2).Co^{II}Pc(-2)]/[Co^{I}Pc(-2)]_2$	$-1.26^{c,d}$	110	$-1.03^{c,d}$	90
$[Co^{I}Pc(-2)]_2/[Co^{I}Pc(-3)]_2$	-2.07	115	-1.90	110
Nap[CoTrNPc]₂				
$[Co^{III}Pc(-1).Co^{III}Pc(-2)]/[Co^{III}Pc(-2)]_2$			0.41^d	

$[Co^{III}Pc(-2)]_2 / [Co^{III}Pc(-2).Co^{II}Pc(-2)]$	-----------		0.29	70
$[Co^{II}Pc(-1)]_2 / [Co^{II}Pc(-1).Co^{II}Pc(-2)]$	0.14	60	-----------	
$[Co^{III}Pc(-2).Co^{II}Pc(-2)] / [Co^{II}Pc(-2)]_2$	-----------		0.05	60
$[Co^{II}Pc(-1).Co^{II}Pc(-2)] / [Co^{II}Pc(-2)]_2$	0.00	70	----------	
$[Co^{II}Pc(-2)]_2 / [Co^{II}Pc(-2).Co^{I}Pc(-2)]$	-0.90	90	-0.87	90
$[Co^{I}Pc(-2).Co^{II}Pc(-2)] / [Co^{I}Pc(-2)]_2$	$-1.29^{c,d}$	100	$-1.09^{c,d}$	150
$[Co^{I}Pc(-2)]_2 / [Co^{I}Pc(-3)]_2$	-2.08	110	-1.97	100

---

a) Potentials are reported with respect to the ferrocenium/ferrocene couple. $E_{1/2}$ values were measured by cyclic voltammetry at 200, 100, 50 and 20 mV/s. Average data being $E = (E_{pa} + E_{pc})/2$ are reported. Data in parenthesis are estimated from overlapping waves. Hatched lines indicate that the Ispecific redox couple is not permissible in that solvent. b) Values of $\triangle E_p = (E_{pa} - E_{pc})$ are given at a potential sweep rate of 50 mV/s, except for those of Nap[CoTrNPc]$_2$ in DMF (20mV/s). c) Irreversible. d) Reported value of $E_{1/2}$ was obtained by differential pulse voltammetry.

Table IV Electronic Spectroscopic Data[a]

Complex	Solvent	Spectroscopic Data (ϵ 10^{-4} L M^{-1} cm^{-1})

Complex	Solvent	Spectroscopic Data
Co(II)TNPc	DMF	326(8.51) 380sh 606(3.89) 668(11.0)
	DCB	330(4.07) 380(1.38) 612(2.57) 678(7.24)
Ant[Co(II)TrNPc]₂	DMF	305(11.77) 327sh 630(8.89) 659(8.71)
	DCB	335sh 393sh 640(7.08) 672(7.41)
[Co(II).Co(I)]	DCB	328sh 432sh 480sh 660(8.12)
[Co(I).Co(I)]	DCB	436sh 472(7.23) 648(3.84) 710(8.93)
[Co(II)Pc(-1)]₂	DCB	363(4.72) 494(2.52) 672(6.36)
Nap[Co(II)TrNPc]₂	DMF	307(10.5) 626(8.07) 675sh(6.89)
	DCB	322sh 388sh 634(7.42) 671(7.01)
[Co(II).Co(I)]	DCB	312(11.0) 440br(2.5) 480sh 650(7.5)
[Co(I).Co(I)]	DCB	308(7.8) 428sh 465(6.5) 642(4.5) 703(7.8)
[Co(II)Pc(-1)]₂	DCB	324(7.3) 400sh 572br(4.0) 680(4.3)
ZnTNPc	DCB	356(8.6) 614(4.0) 680(18.8)
Nap[ZnTrNPc]₂	DMF	281(7.16) 343(13.01) 635(11.6) 672(11.45)
	DCB	340(12.6) 641(11.7) 679(10.9)
Ant[ZnTrNPc]₂	DMF	280(5.09) 342(7.02) 638(6.34) 672(7.79)
	DCB	340(6.08) 643(5.24) 678(5.43)
Nap[Cu(II)TrNPc]₂	DMF	277(5.26) 336(5) 634(6.11) 673(5.23)

DCB 338(5.41)   639(5.81) 678(5.14)

----

a) Data for unelectrolysed species were collected using solutions

$(6-8) \times 10^{-6}$ M in a 10mm cell at 20°C, while those of electrochemically

generated species were obtained using solutions ca 10^{-3} - 10^{-4} M and 1

mm or 0.045 mm OTTLE cells in the presence of ca. 0.3M TBAP

(electrolyte). Note that the presence of electrolyte can influence

the degree of aggregation, as can concentration. Thus spectra obtained

in the presence and in the absence of electrolyte, and at different

concentrations, may not be exactly the same.

Table V

Exciton Splitting, Q Transition Envelope, π Orbital shift, and Ring Oxidation Splitting.

Complex[a]	Solvent	Exciton Splitting cm^{-1}		Half- bandwidth[b] cm^{-1}	Relative Ratio[c]	Q band Max[d] cm^{-1}	π Shift (y)[e] Volts	ΔE[f]
		Uncorr.[g]	Corr.[h]					
Nap[ZnTrNPc]$_2$	DMF	1890	2860	900	1.15	15,750	0.06	0.18
	DCB	1650	3580	2300	1.15	15,650	0.12	0.21
Ant[ZnTrNPc]$_2$	DMF	1690	3300	2025	0.82	15,670	0.10	0.21
	DCB	1700	3470	2480	0.93	15,550	0.11	0.21
EtMeO(5)[ZnTrNPc]$_2$	DCB	2340	3310			15,900	0.06	0.08
ZnTNPc	DCB			650[i]				
Nap[CoTrNPc]$_2$	DMF	2000			1.17	15,970		
	DCB	2250	2730	2700	1.30	15,900	0.03	0.14
Ant[CoTrNPc]$_2$	DMF	1800		2400	1.01	15,870		
	DCB	1750	4000	2520	0.98	15,625	0.14	0.17
Nap[CuTrNPc]$_2$	DMF	2020		2520	1.4			0.27
	DCB	1540		2320	1.35			0.20

EtMeO(5)[CoTrNPc]$_2$ DCB   2450   2450   15,970   0.0   0.0


a) All complexes contain the divalent metal ion. b) Halfbandwidth of
composite Q band envelope measured at half the intensity of the
strongest component, in cm^{-1}. c) Relative ratio of the peak molar
intensities of the shorter to longer wavelength transitions. (NB – this
will vary slightly as a function of concentration and added
electrolyte). d) Higher energy Q band maximum in cm^{-1} e) Variable y
(see text) being the difference between first ring oxidation potential
of mononuclear MTNPc (M = Co or Zn), and the lower component of the
first ring oxidation potential of the binuclear species, in volts. f)
Ring oxidation splitting in volts. g) "Uncorrected" Q band exciton
splitting, measured according to method in the text, in cm^{-1}. h)
"Corrected" exciton coupling obtained from sum of the "uncorrected"
value plus 2y (expressed in cm^{-1} by multiplying the volt value by 8065)
and rounded off to the nearest 10 cm^{-1}. i) Halfbandwidth of the Q band
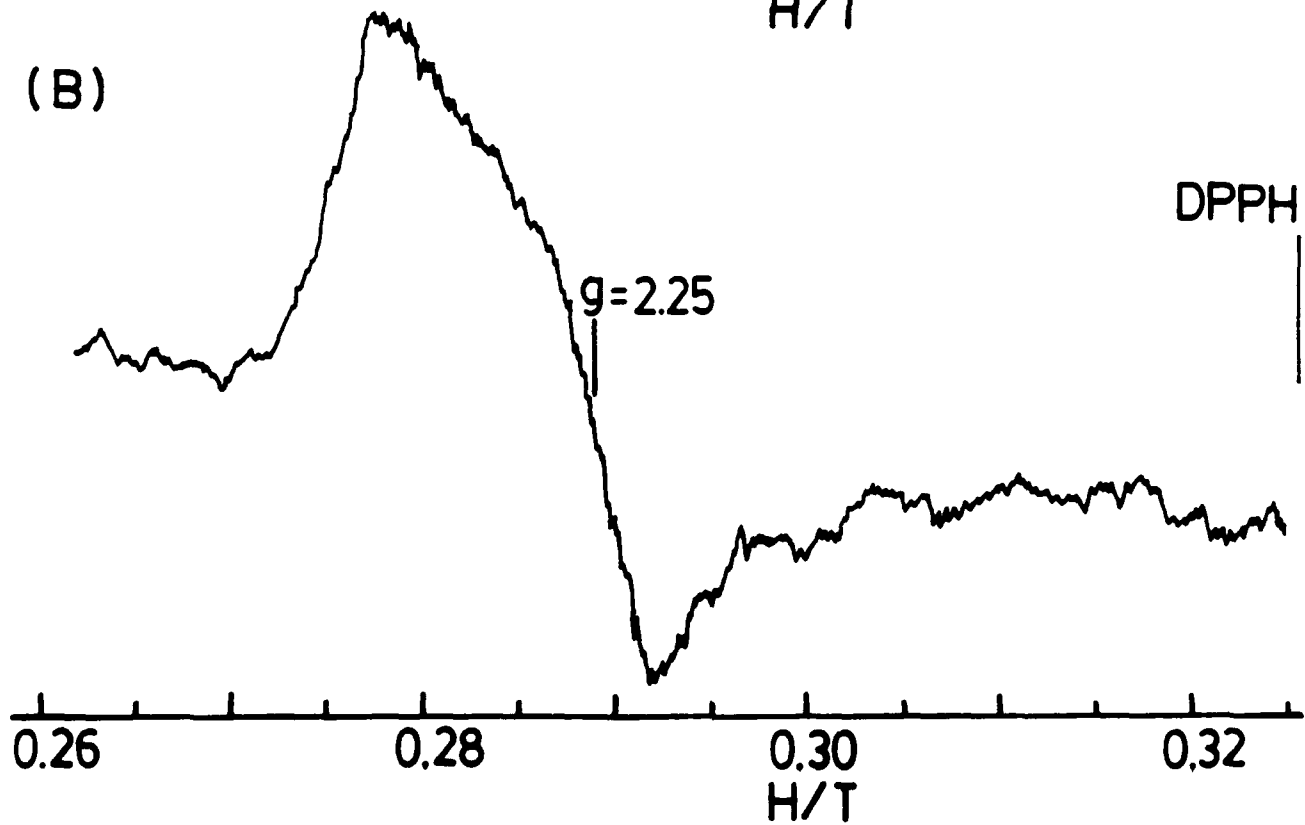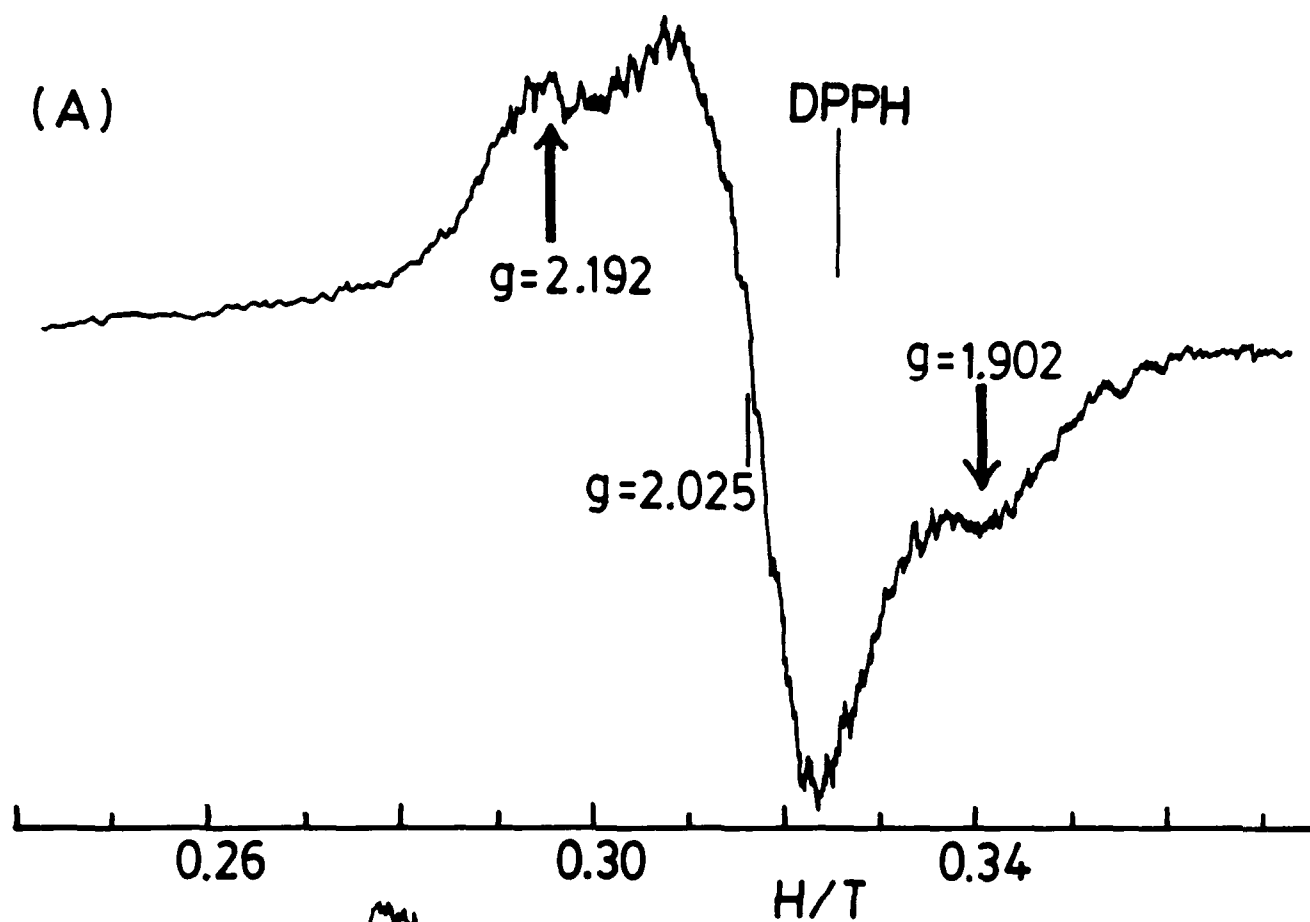in monomeric ZnTNPc from data in ref.8g, in cm^{-1}.
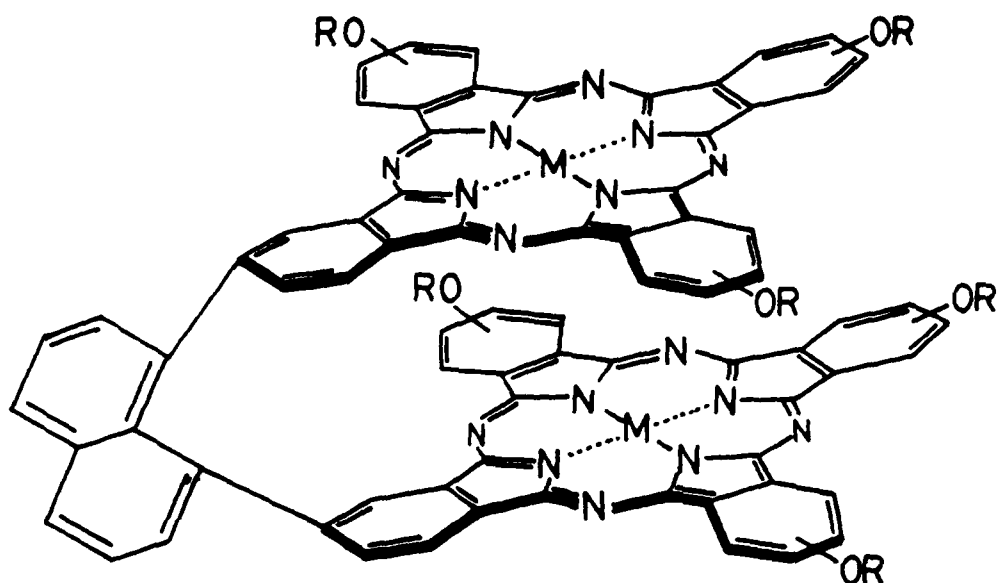
Nap[ZnTrNPc]$_2$: M=Zn, R=CH$_2$C(CH$_3$)$_3$
Nap[CoTrNPc]$_2$: M=Co, R=CH$_2$C(CH$_3$)$_3$
Nap[CuTrNPc]$_2$: M=Cu, R=CH$_2$C(CH$_3$)$_3$
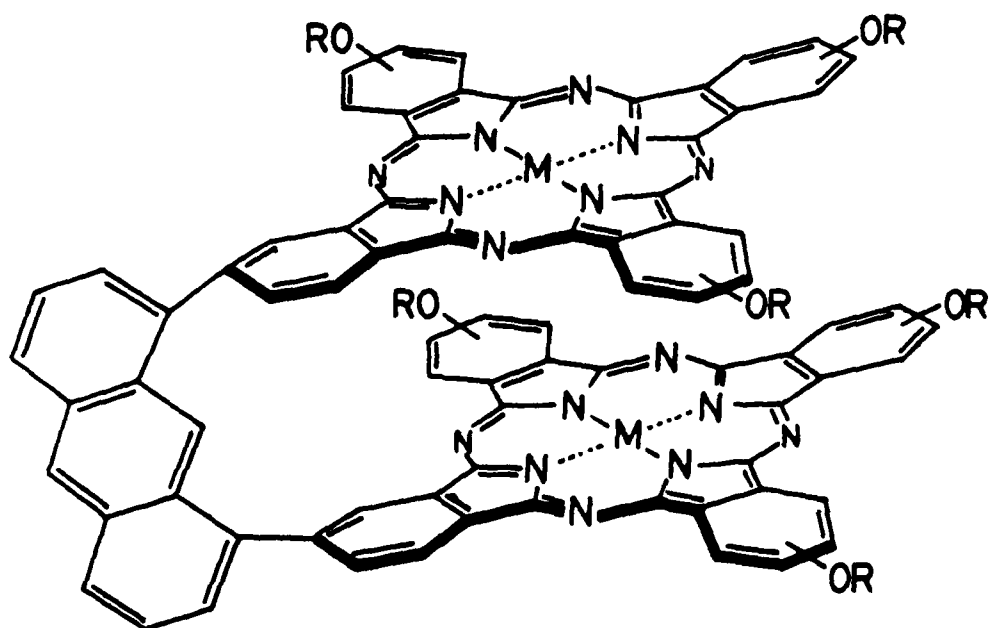
Ant[ZnTrNPc]$_2$: M=Zn, R=CH$_2$C(CH$_3$)$_3$
Ant[CoTrNPc]$_2$: M=Co, R=CH$_2$C(CH$_3$)$_3$
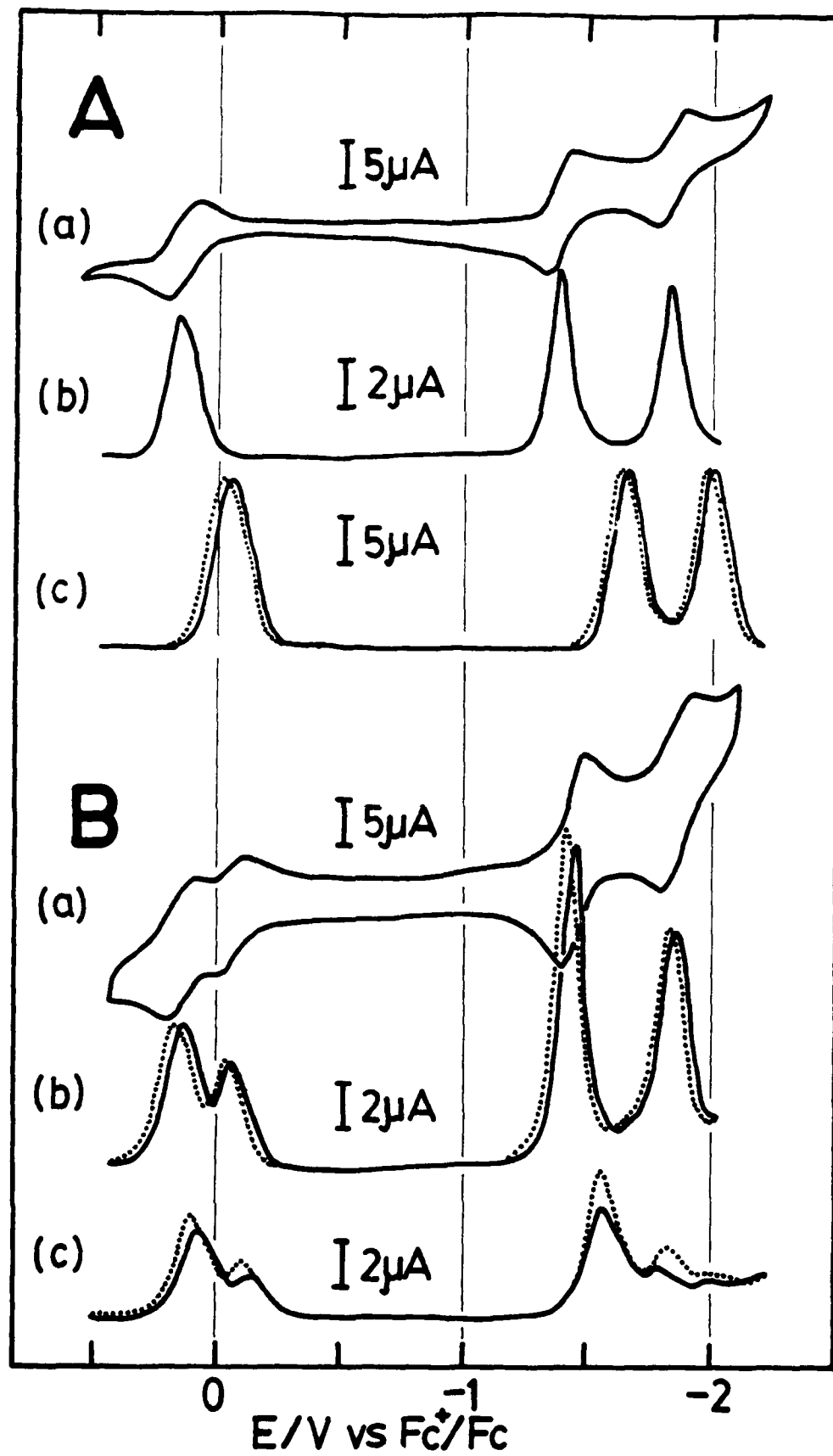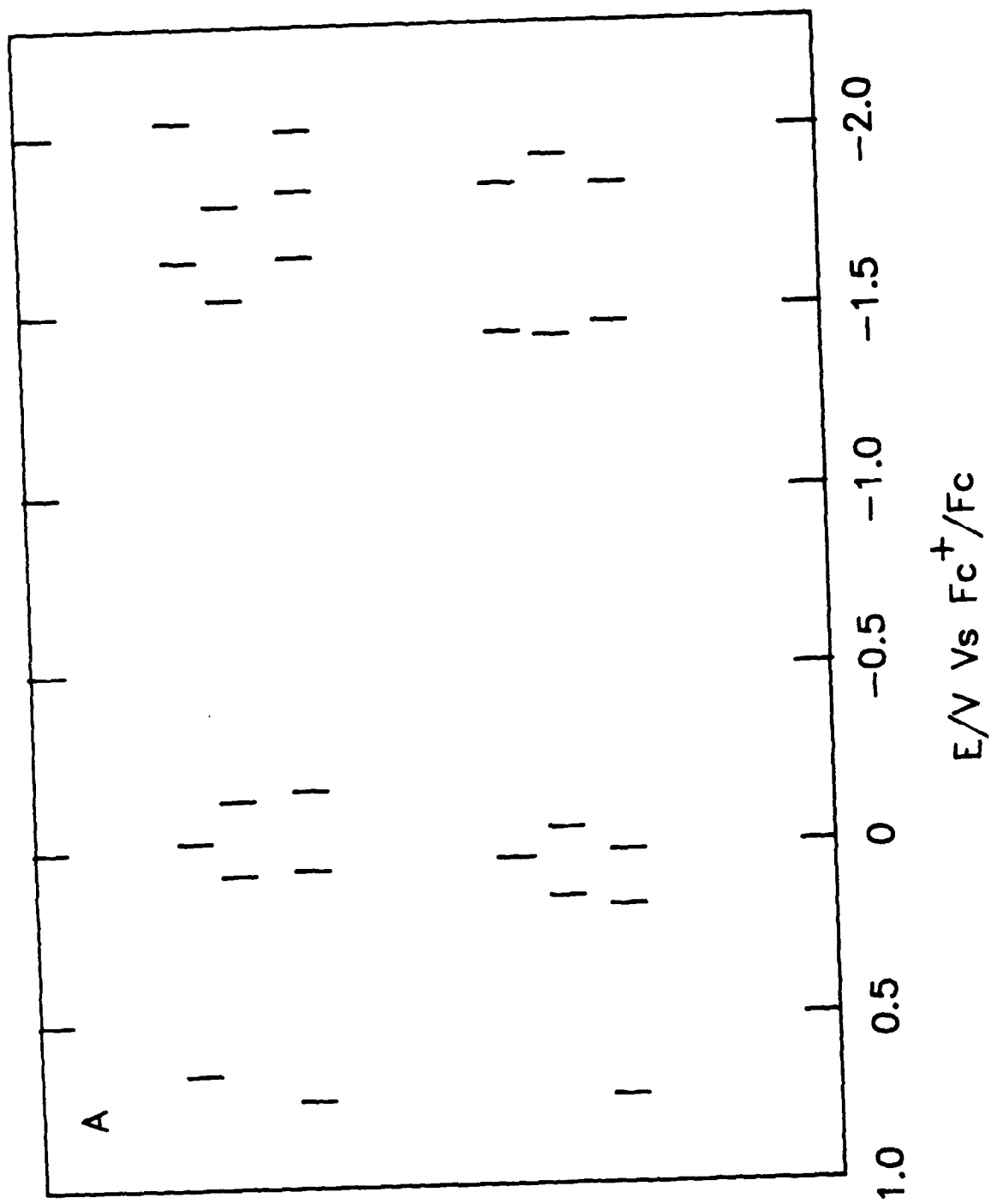
A

(a) $I\,5\mu A$

(b) $I\,2\mu A$

(c) $I\,5\mu A$

B

(a) $I\,5\mu A$

(b) $I\,2\mu A$

(c) $I\,2\mu A$

0   −1   −2

E/V vs Fc/Fc^{+}

Fig. 3 N. Koiⁱⁱⁱⁱ et al.

A

DCB

ZnTNPc
Ant[ZnTrNPc]₂
Nap[ZnTrNPc]₂

DMF

Ant[ZnTrNPc]₂
Nap[ZnTrNPc]₂

E/V Vs Fc$^+$/Fc

F, 4A 4B KONOTOSU)

B

DCB
CoTNPc
Ant[CoTrNPc]$_2$
Nap[CoTrNPc]$_2$

DMF
CoTNPc
Ant[CoTrNPc]$_2$
Nap[CoTrNPc]$_2$

1.0   0.5   0   -0.5   -1.0   -1.5   -2.0

E/V Vs Fc$^+$/Fc

Fig. 46. Kolawole, John

Fig 5
KOBAYASHI

A

L⁺/L   Co^III/II   Co^II/I   L/L⁻

200
100
50

I5µA

I5µA

100
50

B

5

I2µA

0   −1   −2

E/V vs Fc⁺/Fc

Fig 6

A

B

0.1 a.u

300   400   500   600   700   800
Wavelength/nm

Fig. 7

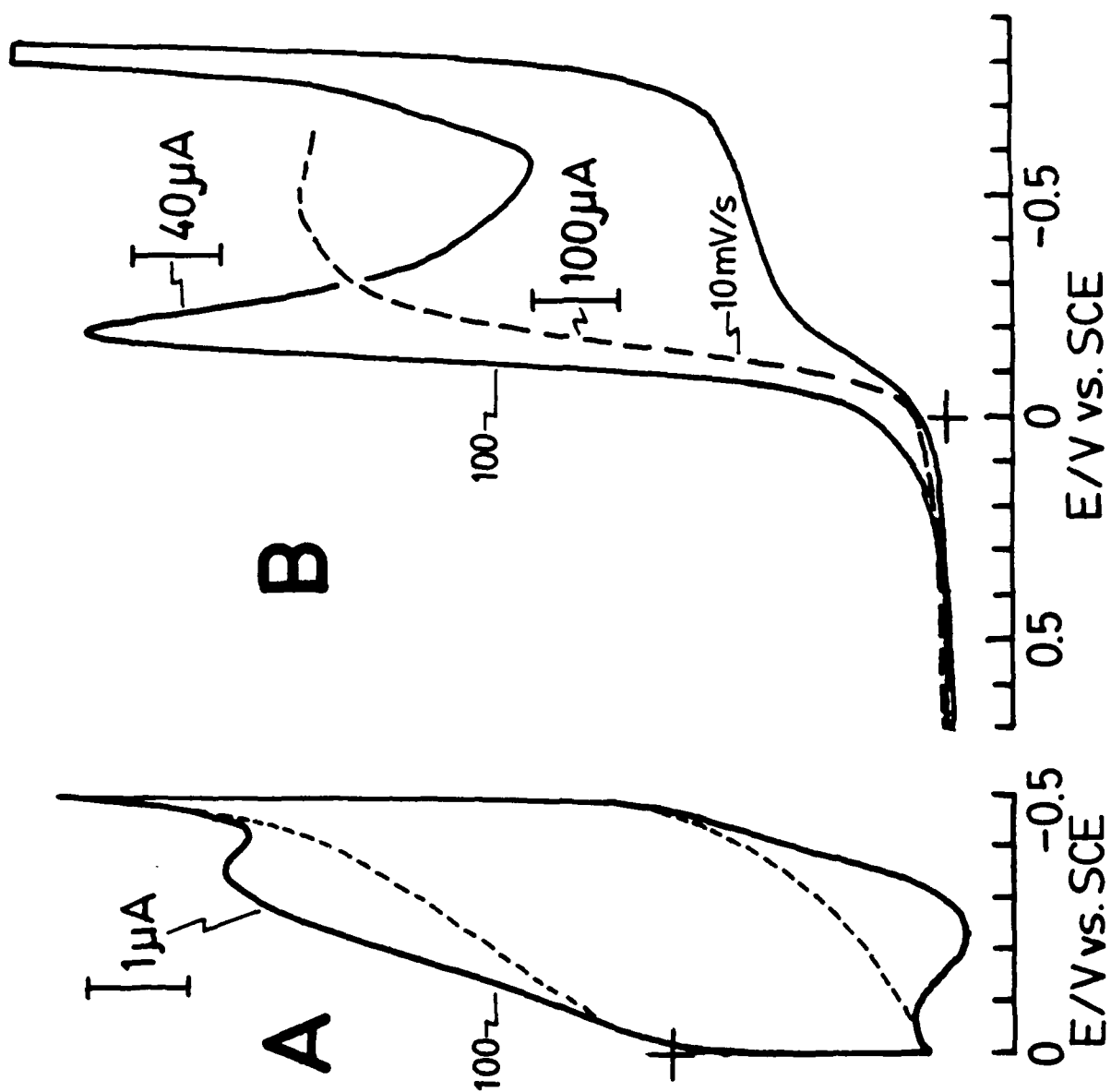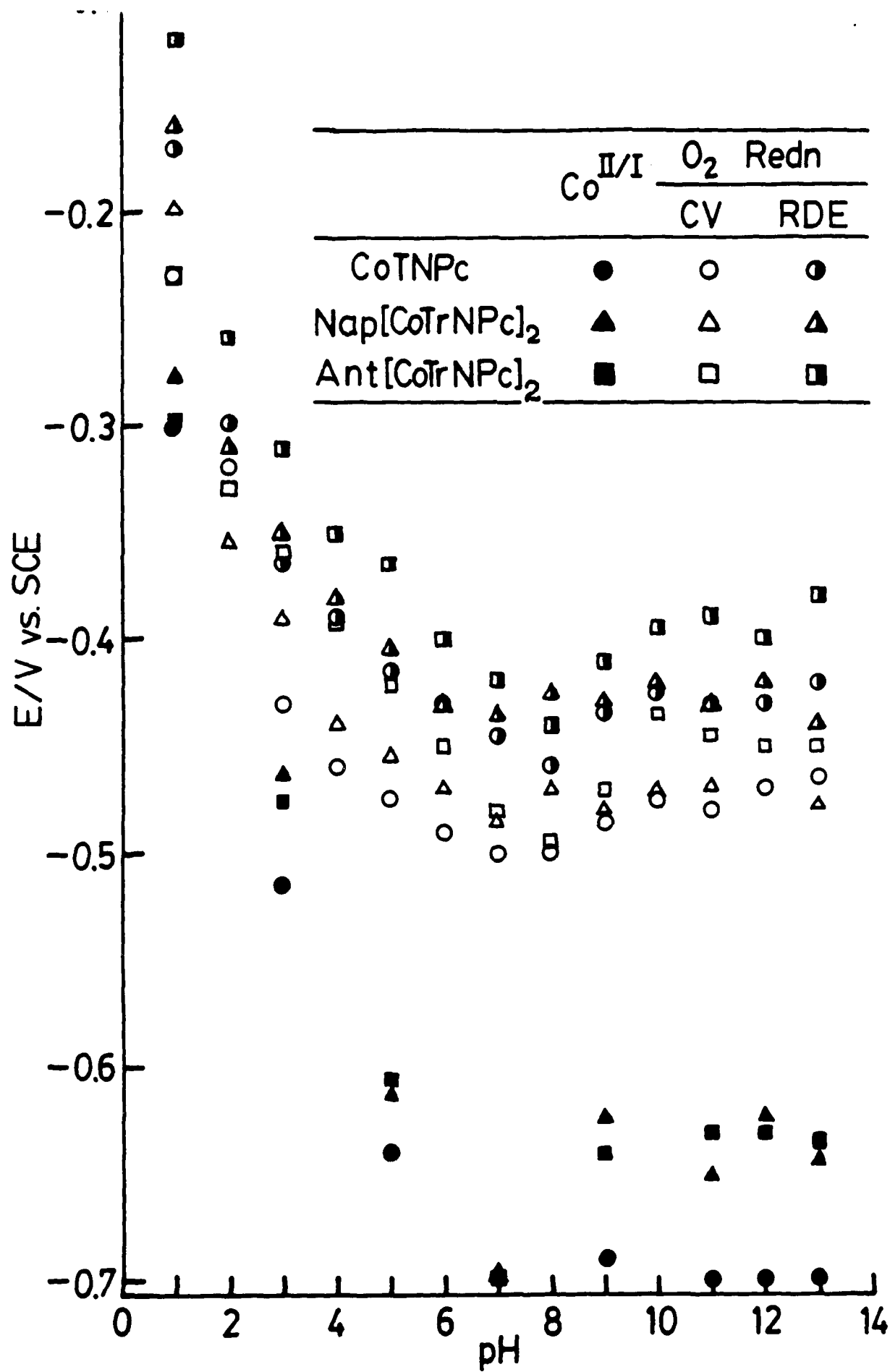Wavelength/nm

π*E$_g$

πA1u

E$_g$

A1u

g

u

u

g

Y1
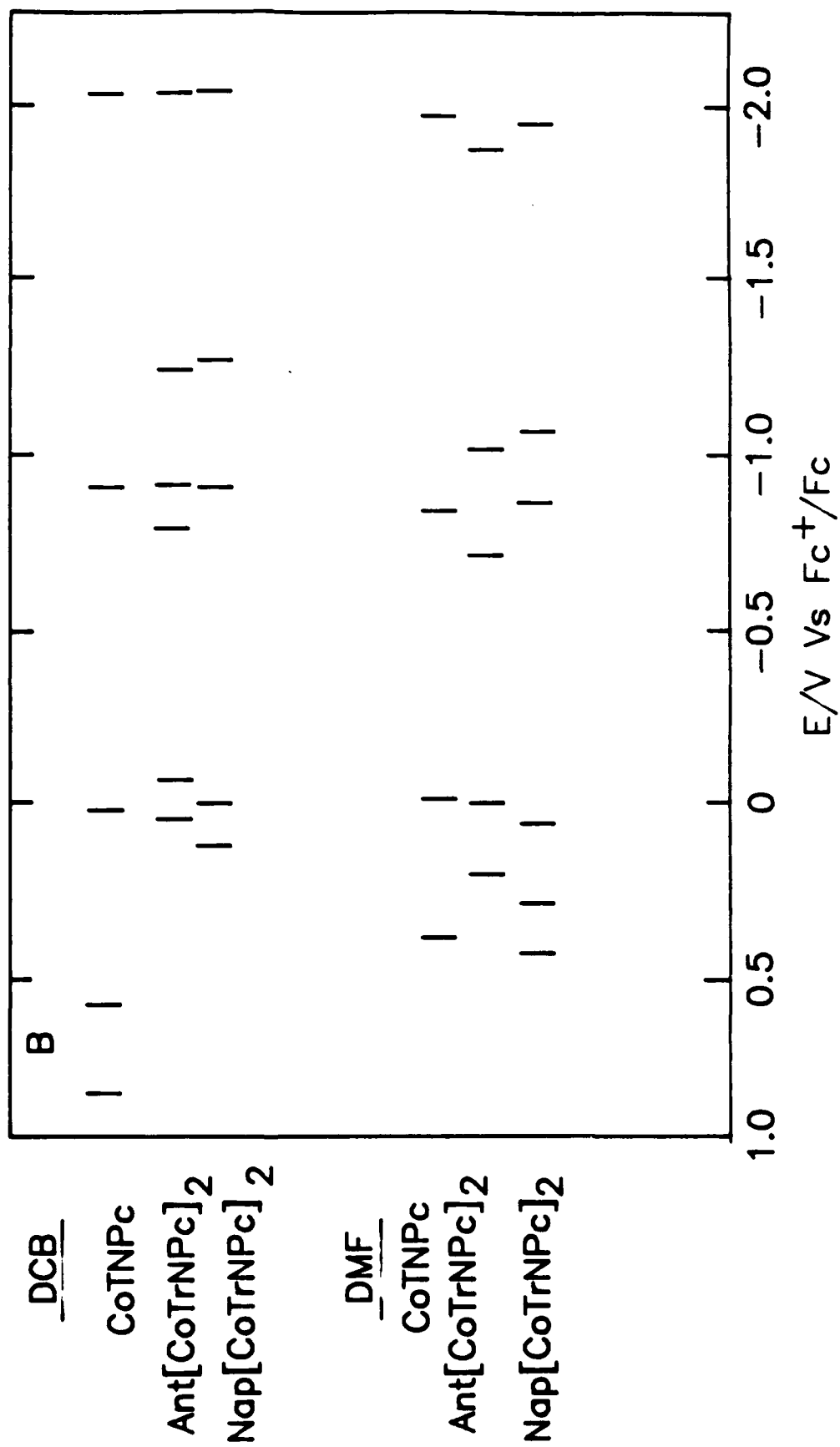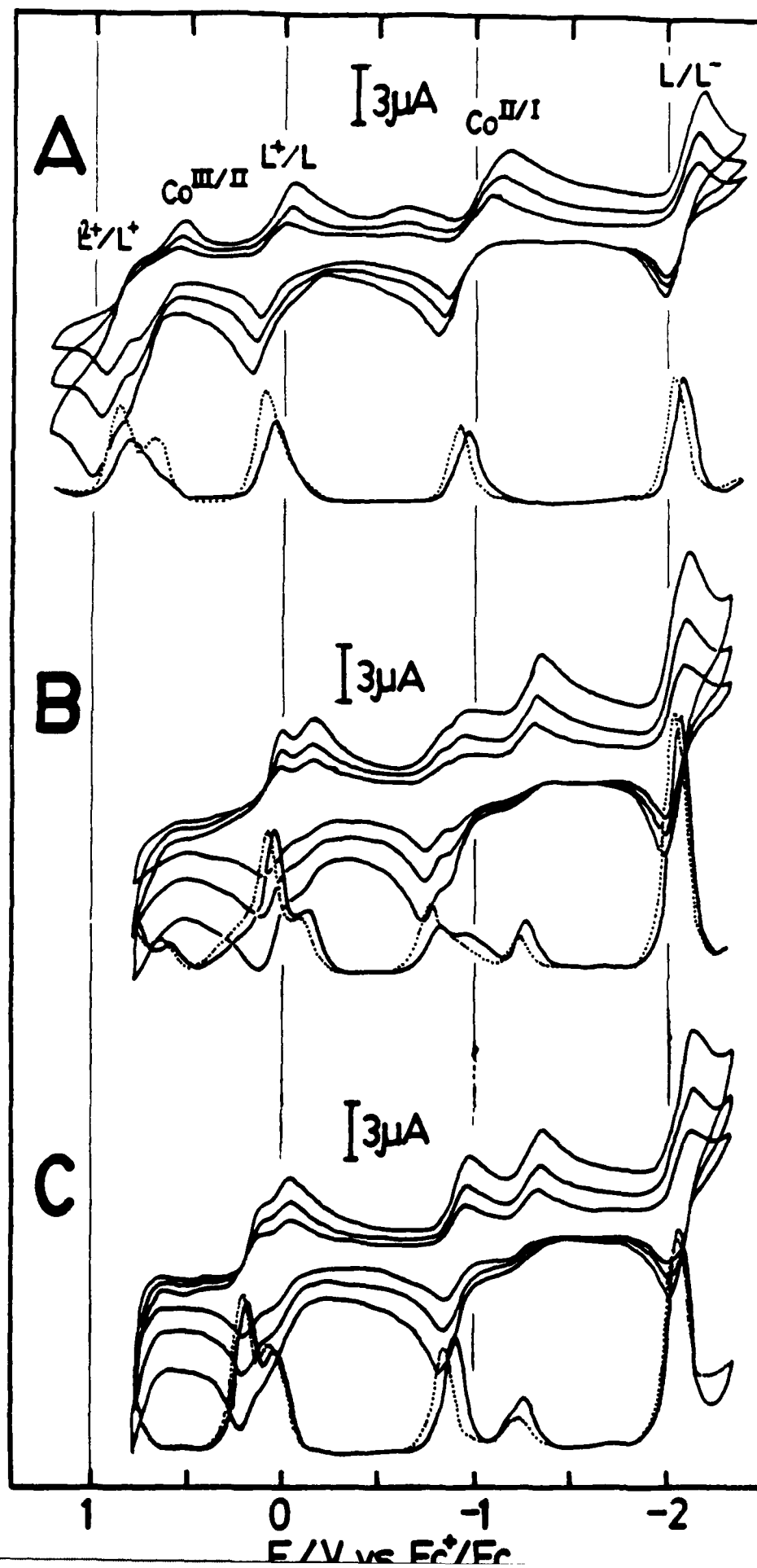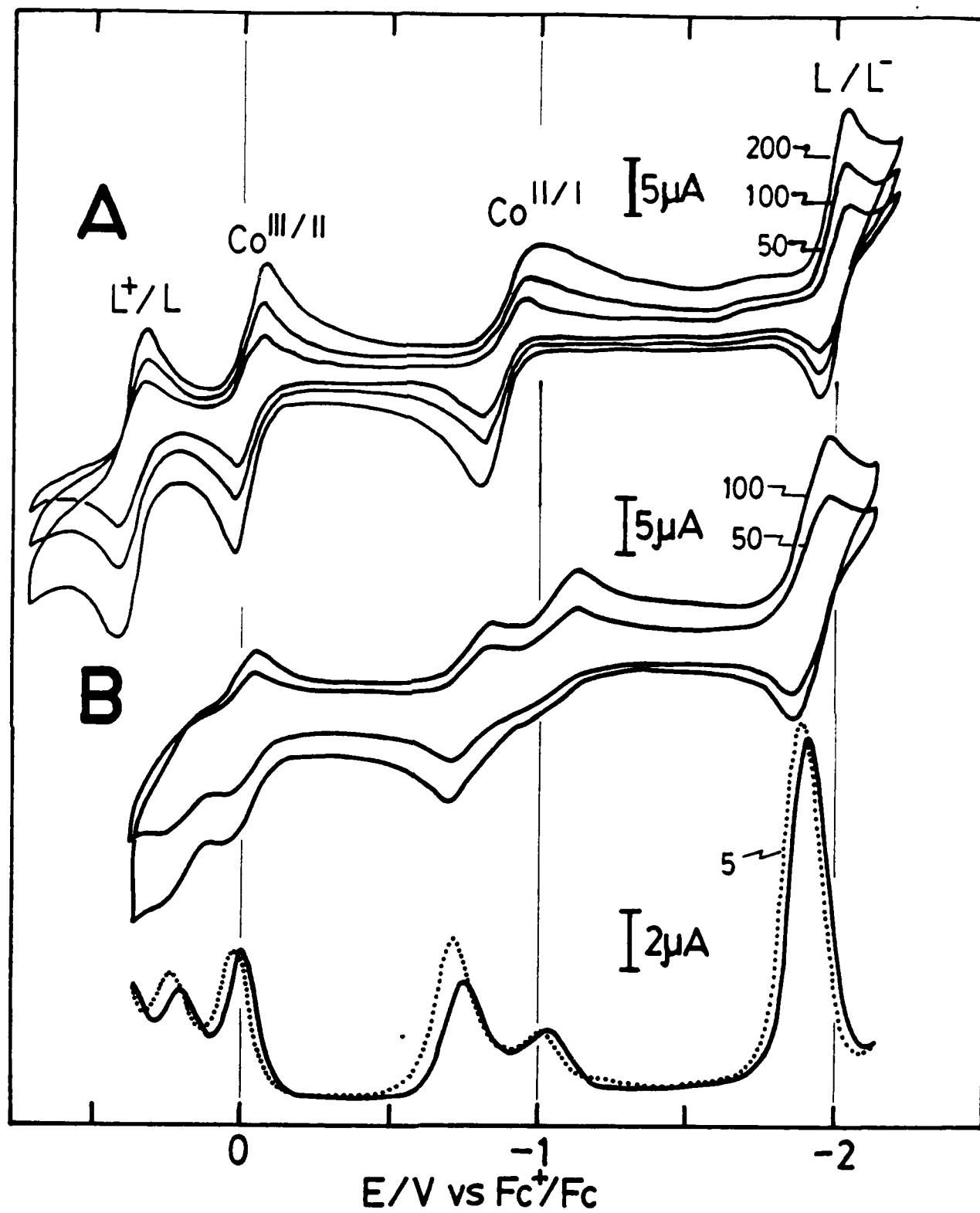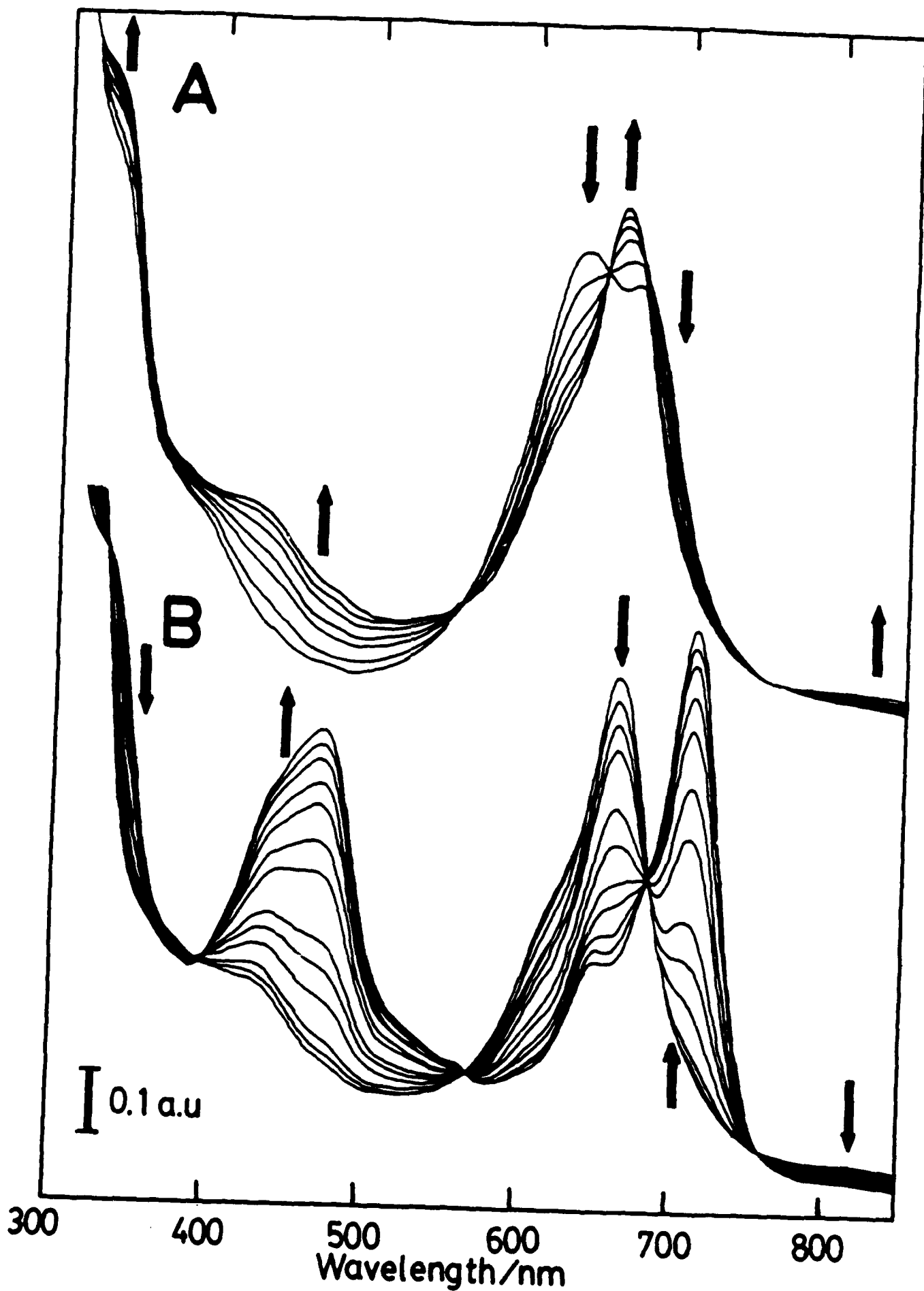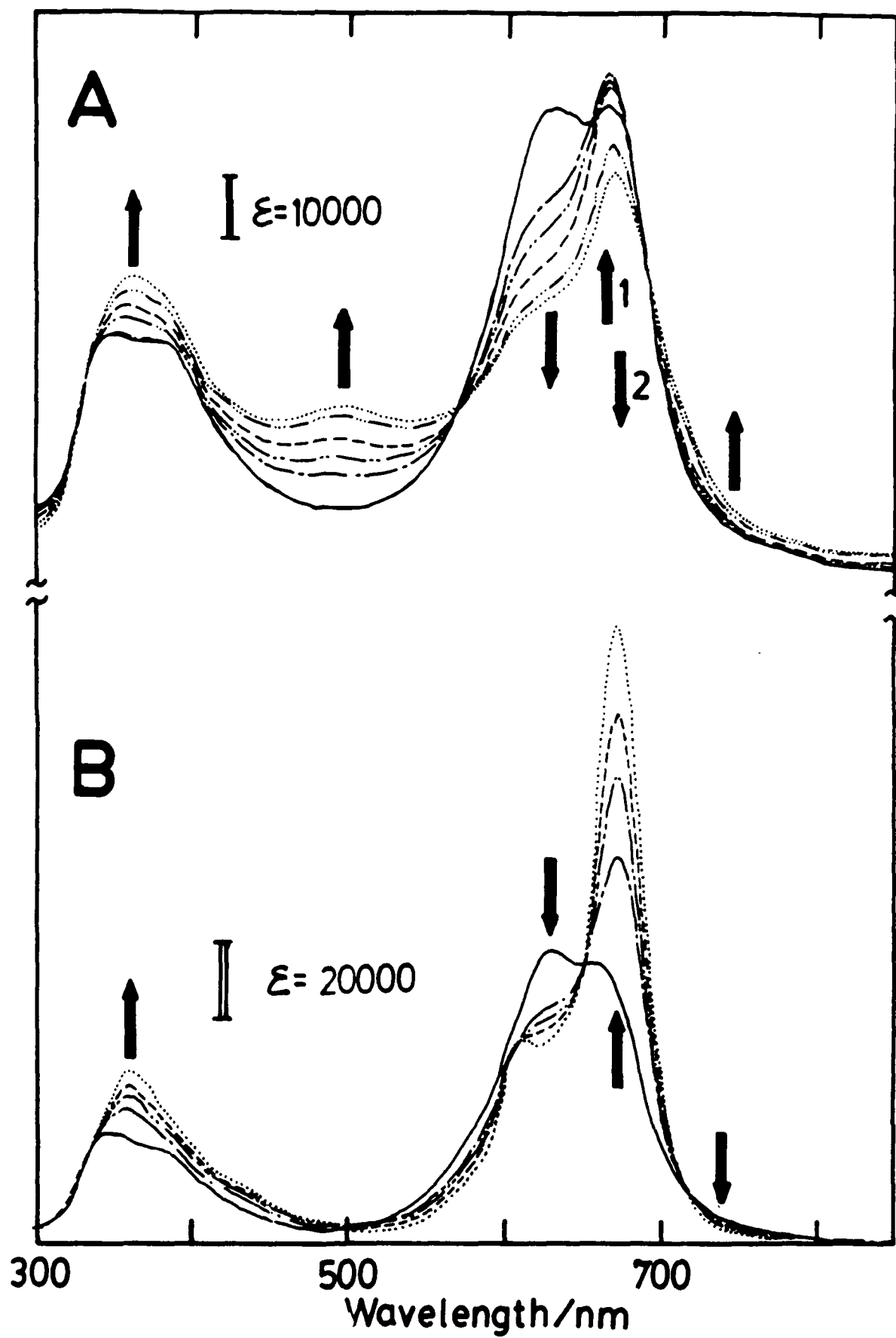
Fig. 13 N. Kobayashi et al.

Fig. 11 N. Kobayashi et al